AD-A136 434 AN INVESTIGATION OF METHODS FOR COMPUTING LONG PATH ATMOSPHERIC TRANSMITT..(U) AEROSPACE CORP EL SEGUNDO CA CHEMISTRY AND PHYSICS LAB B R JOHNSON 01 DEC 83 1/1

UNCLASSIFIED TR-0084(4753-08)-1 SD-TR-83-82 F/G 4/1 NL

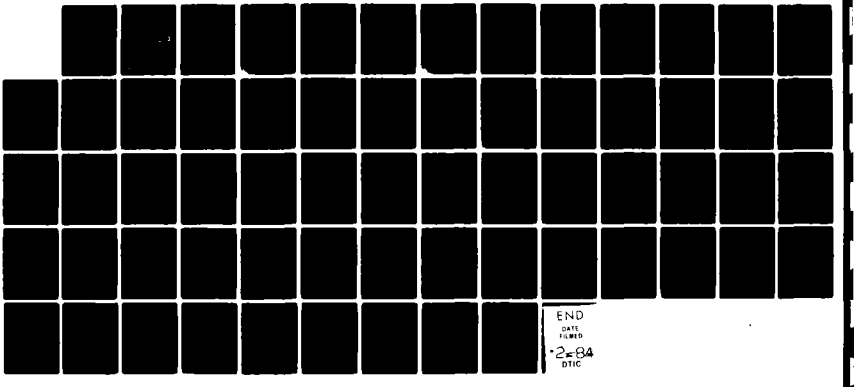

END
DATE FILMED
2-84
DTIC

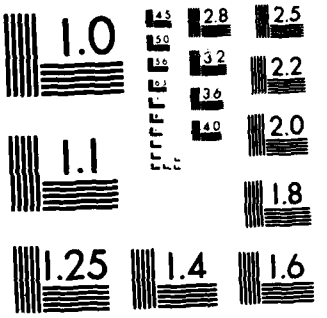

An Investigation of Methods for Computing Long Path Atmospheric Transmittance

B. R. JOHNSON
Chemistry and Physics Laboratory
Laboratory Operations
The Aerospace Corporation
El Segundo, Calif. 90245

1 December 1983

APPROVED FOR PUBLIC RELEASE;
DISTRIBUTION UNLIMITED

Sponsored by
DEFENSE ADVANCED RESEARCH PROJECTS AGENCY (DOD)
DARPA Order No. 2965
Monitored by SD Under Contract No. F04701-83-C-0084
SPACE DIVISION
AIR FORCE SYSTEMS COMMAND
Los Angeles Air Force Station
P.O. Box 92960, Worldway Postal Center
Los Angeles, Calif. 90009

THE VIEWS AND CONCLUSIONS CONTAINED IN THIS DOCUMENT ARE THOSE OF THE AUTHORS AND SHOULD NOT BE INTERPRETED AS NECESSARILY REPRESENTING THE OFFICIAL POLICIES, EITHER EXPRESSED OR IMPLIED, OF THE DEFENSE ADVANCED RESEARCH PROJECTS AGENCY OR THE U.S. GOVERNMENT.

This report was submitted by The Aerospace Corporation, El Segundo, CA 90245, under Contract No. F04701-83-C-0084 with the Space Division, P.O. Box 92960, Worldway Postal Center, Los Angeles, CA 90009. It was reviewed and approved for The Aerospace Corporation by S. Feuerstein, Director, Chemistry and Physics Laboratory. Capt. Ronald C. Lawson, SD/YGD, was the Air Force project officer. This research was supported by the Defense Advanced Research Projects Agency of the Department of Defense.

This report has been reviewed by the Public Affairs Office (PAS) and is releasable to the National Technical Information Service (NTIS). At NTIS, it will be available to the general public, including foreign nationals.

This technical report has been reviewed and is approved for publication. Publication of this report does not constitute Air Force approval of the report's findings or conclusions. It is published only for the exchange and stimulation of ideas.

Ronald C. Lawson

Ronald C. Lawson, Capt. USAF
Chief, Orbital Operations Division
Defense Support Program

Joseph Hess

Joseph Hess, GM-15, Director
West Coast Office, Air Force Space
Technology Center

UNCLASSIFIED

SECURITY CLASSIFICATION OF THIS PAGE (When Data Entered)

REPORT DOCUMENTATION PAGE	READ INSTRUCTIONS BEFORE COMPLETING FORM
1. REPORT NUMBER: SD-TR-83-82	2. GOVT ACCESSION NO.: AD-A136434
3. RECIPIENT'S CATALOG NUMBER	
4. TITLE (and Subtitle): AN INVESTIGATION OF METHODS FOR COMPUTING LONG PATH ATMOSPHERIC TRANSMITTANCE	5. TYPE OF REPORT & PERIOD COVERED
6. PERFORMING ORG. REPORT NUMBER: TR-0084(4753-08)-1	
7. AUTHOR(s): Bernard R. Johnson	8. CONTRACT OR GRANT NUMBER(s): F04701-83-C-0084
9. PERFORMING ORGANIZATION NAME AND ADDRESS: The Aerospace Corporation, El Segundo, California 90245	10. PROGRAM ELEMENT, PROJECT, TASK AREA & WORK UNIT NUMBERS
11. CONTROLLING OFFICE NAME AND ADDRESS: Defense Advanced Research Projects Agency, 1400 Wilson Blvd, Arlington, VA 22209	12. REPORT DATE: 1 December 1983
	13. NUMBER OF PAGES: 56
14. MONITORING AGENCY NAME & ADDRESS (if different from Controlling Office): Space Division, Los Angeles Air Force Station, Los Angeles, California 90009	15. SECURITY CLASS. (of this report): Unclassified
	15a. DECLASSIFICATION/DOWNGRADING SCHEDULE

16. DISTRIBUTION STATEMENT (of this Report)

Approved for public release; distribution unlimited.

Accession For
NTIS GRA&I
DTIC TAB
Unannounced
Justification
By
Distribution/
Availability Codes
Dist Avail and/or Special
A-1

17. DISTRIBUTION STATEMENT (of the abstract entered in Block 20, if different from Report)

18. SUPPLEMENTARY NOTES

19. KEY WORDS (Continue on reverse side if necessary and identify by block number)

Atmospheric Transmittance
Attenuation
Band Model
Infrared
Long Path Transmittance

DTIC

20. ABSTRACT (Continue on reverse side if necessary and identify by block number)

The reliability of the statistical band model for long path length, low transmittance conditions is investigated by comparing the band model with precise line by line calculations. Two test systems are utilized; a system of H_2O absorbers and a system of computer generated line parameters. It is found that the statistical band model is fairly reliable for calculating band transmittance in the range $\bar{T} > 0.1$, but for transmittance less than this, it is not reliable and can be in error by several orders of magnitude. An explanation for this behavior is offered.

DD FORM 1473 (FACSIMILE)

UNCLASSIFIED

SECURITY CLASSIFICATION OF THIS PAGE (When Data Entered)

19. KEY WORDS (Continued)

20. ABSTRACT (Continued)

In the second part of this investigation, a new nonstatistical method based on a simple approximation of the k-distribution function is developed. It is compared with precise line by line calculations and is found to be very reliable for all transmittance conditions.

CONTENTS

I. INTRODUCTION..... 5

II. COMPARISON OF STATISTICAL BAND MODEL AND LINE BY LINE TRANSMITTANCE..... 7

A. H_2O Line Parameters..... 8

B. H_2O Line Parameter Distribution..... 13

C. Computer Generated Line Parameters..... 15

III. NEW TRANSMITTANCE APPROXIMATIONS..... 27

A. Two-Parameter Approximation..... 28

B. Three-Parameter Approximation..... 35

C. k-Distribution Function..... 41

D. Monte Carlo Method..... 50

IV. SUMMARY AND DISCUSSION..... 55

REFERENCES..... 57

FIGURES

1. Comparison of Line by Line ($\overline{T}_L$) and Band Model ($\overline{T}_B$) Transmittances at 30 km..... 10

2. Comparison of Line by Line ($\overline{T}_L$) and Band Model ($\overline{T}_B$) Transmittances for 3040 cm^{-1} Band..... 11

3. Comparison of Line by Line ($\overline{T}_L$) and Band Model ($\overline{T}_B$) Transmittances for 3060 cm^{-1} Band..... 12

4. Stick Diagram or H_2O Line Spectrum in the 3040 and 3060 cm^{-1} Bands..... 14

5. Line Strength Distribution..... 16

6. Line Spacing Distribution..... 17

7. Line Width Distribution..... 18

8. Spectral Absorption Coefficient k(ν) in the 3040 and 3060 cm^{-1} Bands..... 19

9. Stick Diagram of a Computer Generated Line Spectrum..... 22

10. Line Strength Distribution for the Computer Generated Lines..... 22

11. Line Spacing Distribution for the Computer Generated Lines..... 23

12. Spectral Absorption Coefficient k(ν), Obtained from the Computer Generated Lines..... 23

13. Comparison of Line by Line ($\overline{T}_L$) and Band Model ($\overline{T}_B$) Transmittances Obtained from Computer Generated Lines..... 24

14. Ensemble of 20 Band Model Curves from 20 Random Samples of Computer Generated Line Parameters..... 25

15. Monotonic Absorption Function k(p)..... 29

16. Comparison of Line by Line ($\overline{T}_L$) and Two-Parameter Model ($\overline{T}_2$) Transmittances for 3040 cm^{-1} Band..... 32

FIGURES (Continued)

17. Comparison of Line by Line ($\overline{T}_L$) and Two-Parameter Model ($\overline{T}_2$) Transmittances for 3060 cm^{-1} Band..... 33

18. Monotonic Absorption Function k(p)..... 36

19. Comparison of Line by Line ($\overline{T}_L$) and Alternate Two-Parameter Model ($\overline{T}_2$) Transmittances for the 3040 cm^{-1} Band..... 37

20. Comparison of Line by Line ($\overline{T}_L$) and Alternate Two-Parameter Model ($\overline{T}_2$) Transmittances for the 3060 cm^{-1} Band..... 38

21. Monotonic Absorption Function k(p)..... 40

22. Comparison of Line by Line ($\overline{T}_L$) and Three-Parameter Model ($\overline{T}_3$) Transmittances for 3040 cm^{-1} Band..... 42

23. Comparison of Line by Line ($\overline{T}_L$) and Three-Parameter Model ($\overline{T}_3$) Transmittances for 3060 cm^{-1} Band..... 43

24. k-Distribution Functions..... 45

25. k-Distribution Functions..... 46

26. Monotonic Absorption Function..... 48

27. Comparison of Line by Line ($\overline{T}_L$) and 50 Point Monte Carlo ($\overline{T}_{50}$) Transmittances for 3040 cm^{-1} Band..... 53

28. Comparison of Line by Line ($\overline{T}_L$) and 50 Point Monte Carlo ($\overline{T}_{50}$) Transmittances for 3060 cm^{-1} Band..... 54

FIGURES (Continued)

17. Comparison of Line by Line ($\overline{T}_L$) and Two-Parameter Model ($\overline{T}_2$) Transmittances for 3060 cm^{-1} Band..... 33

18. Monotonic Absorption Function k(p)..... 36

19. Comparison of Line by Line ($\overline{T}_L$) and Alternate Two-Parameter Model ($\overline{T}_2$) Transmittances for the 3040 cm^{-1} Band..... 37

20. Comparison of Line by Line ($\overline{T}_L$) and Alternate Two-Parameter Model ($\overline{T}_2$) Transmittances for the 3060 cm^{-1} Band..... 38

21. Monotonic Absorption Function k(p)..... 40

22. Comparison of Line by Line ($\overline{T}_L$) and Three-Parameter Model ($\overline{T}_3$) Transmittances for 3040 cm^{-1} Band..... 42

23. Comparison of Line by Line ($\overline{T}_L$) and Three-Parameter Model ($\overline{T}_3$) Transmittances for 3060 cm^{-1} Band..... 43

24. k-Distribution Functions..... 45

25. k-Distribution Functions..... 46

26. Monotonic Absorption Function..... 48

27. Comparison of Line by Line ($\overline{T}_L$) and 50 Point Monte Carlo ($\overline{T}_{50}$) Transmittances for 3040 cm^{-1} Band..... 53

28. Comparison of Line by Line ($\overline{T}_L$) and 50 Point Monte Carlo ($\overline{T}_{50}$) Transmittances for 3060 cm^{-1} Band..... 54

I. INTRODUCTION

A line by line calculation is the most accurate and general means for computing the atmospheric transmission of radiant energy. With the aid of a modern computer and the recent convenient availability of tables of line parameters stored on magnetic tape,[1] such calculations can now be routinely carried out.

For many applications, the quantity of interest is the mean value of the transmittance over a band interval $\Delta\nu$

$$\bar{T} = \frac{1}{\Delta\nu} \int_{\Delta\nu} T(\nu)\, d\nu \qquad (1)$$

The total numerical effort required to compute $\bar{T}$ using the line by line method is quite large and any extensive calculation of mean transmittance values can be quite time consuming, even on a fast computer.

Band model theory, on the other hand, provides a simple parameterized formula for computing the mean band transmittance, which is much more efficient than the line by line calculations. However, since it is based on certain simplifying assumptions it must be tested for accuracy. Previous studies[2] comparing the statistical band model with line by line calculations have shown a reasonable agreement between the two methods. This comparison, however, was carried out for small to moderate optical path distances where the transmittances were in the range $\bar{T} = > 0.1$. Comparisons have not been made in the very long path length regime where $\bar{T} < 0.1$. In this report, we present the results of such a comparison. The details are given in Section II.

We will conclude from this comparison that the band model does not, in general, give very good results in the regime where $\bar{T} = < 0.1$. In fact, as

[1] L. S. Rothmon, Appl. Opt. 20, 791 (1981).
[2] A. Goldman and T. Kyle, Appl. Opt. 7, 1167 (1968).

will be seen, the transmittance can be in error by several orders of magnitude and is shown to have the wrong asymptotic behavior as the optical path length approaches infinity.

In Section III, we derive new parameterized formulas for computing the mean band transmittance $\bar{\tau}(x)$. These formulas are accurate for all values of optical distance x, including the limit as x approaches infinity. The results of comparisons with both the precise line by line calculations and statistical band model calculations will also be presented.

Section IV is a summary and discussion.

II. COMPARISON OF STATISTICAL BAND MODEL AND LINE ..INE TRANSMITTANCE

The line parameter data for these calculations were obtained from the Air Force Geophysics Laboratory (AFGL) line atlas.[1] This compilation provides data for seven gas species: H_2O, CO_2, O_3, N_2O, CH_4, CO, and O_2. The data given for each line include the line position λ_i (cm^{-1}), the line strength S_1^0 (cm^{-1}/molecule - cm^{-2} at 296°K), the line half-width γ_i^0 (cm^{-1} for air broadening at 296°K and 1 atm pressure), and the energy of the lower level of the transition E_i (cm^{-1}). The subscript i labels the line, while the superscript 0 on the strength S_i^0 and the half-width γ_i^0 indicate that these quantities are taken directly from the atlas and are, therefore, appropriate for a pressure of 1 atm and temperature of 296°K.

The line strength S_i and the width parameter γ_i at any other temperature and pressure are computed from S_i^0 and γ_i^0 using the same formulas employed by C. M. Randall in his general line by line computer program, INHOM. A discussion of these formulas is given in Ref. 3.

All calculations have been carried out assuming a Lorentz pressure broadened line shape function. The spectral absorption coefficient is given by

$$k(\nu) = \frac{1}{\pi} \sum_i \frac{n_i S_i \gamma_i}{(\nu - \nu_i)^2 - \gamma_i^2} \tag{2}$$

The quantity n_i is the density of the gas for which S_i and γ_i characterize a line. The units of n_i used in this study are molecules/(cm^2 - km), i.e., the number of molecules in a column 1 km long and 1 cm^2 in cross sectional area. By including the density factor n_i in the definition, $k(\nu)$ has the convenient dimension 1/km. The transmittance at wave number ν is given by

$$T(\nu, x) = \exp [-k(\nu) x] \tag{3}$$

---

[3] S. J. Young, Band Model Parameters for the 2.7-μm Bands of H_2O and CO_2 in the 100 to 3000°K Temperature Range, TR-0076(6970)-4, The Aerospace Corp. (31 July 1975).

where x is the distance measured in kilometers. The mean band transmittance is then computed by averaging $T(\nu,x)$ over the band interval $\Delta\nu$ [see Eq. (1)]

$$\bar{T}(x) = \frac{1}{\Delta\nu} \int_{\Delta\nu} \exp\,[-k(\nu)\,x]d\nu \tag{4}$$

In the statistical band model with exponential-tailed inverse line strength distribution,[4] the mean band transmittance is given by[3,4]

$$\bar{T}(x) = \exp\left[-\frac{2\bar{\gamma}}{\delta_e}\left(1 + \frac{\bar{k}\,\delta_e}{\bar{\gamma}}\,x - 1\right)\right] \tag{5}$$

where $\bar{k}$, δ_e, and $\bar{\gamma}$ are the three band model parameters. The band model parameters can be expressed as certain averages of the line parameters over the spectral interval $\Delta\nu$. The parameter $\bar{k}$ is defined by the expression

$$\bar{k} = \frac{1}{\Delta\nu} \sum_{i=1}^{L} n_i\,S_i \tag{6}$$

where L is the number of lines in the interval $\Delta\nu$. The parameter $\bar{\gamma}$ is the average line width

$$\bar{\gamma} = \frac{1}{L} \sum_{i=1}^{L} \gamma_i \tag{7}$$

and δ_e is a measure of the effective average distance between lines in $\Delta\nu$

$$\frac{1}{\delta_e} = \frac{1}{\bar{k}\,\bar{\gamma}} \left[\frac{1}{\Delta\nu} \sum_{i=1}^{L} n_i\,S_i\,\gamma_i\right]^2 \tag{8}$$

A. H_2O LINE PARAMETERS

The model system used for the calculations in this report has the following specifications: pressure, 1013 mbar; temperature, 300°K; concentration of H_2O, 0.026; concentration of O_2, 0.21. The wave number range in which the calculations are carried out is 2800 to 3400 cm^{-1}. (Only the H_2O molecules

[4] W. Malkmus, J. Opt. Soc. Am. 57, 323 (1967).

have absorption lines in this range; the O_2 concentration is specified because of its influence on the width parameters of the H_2O lines.) The density n of H_2O molecules in this model system is

$$n = 6.36 \times 10^{22} \frac{\text{molecules}}{\text{cm}^2 - \text{km}} \tag{9}$$

The spectral band interval is chosen to be $\Delta\nu = 20$ cm^{-1}. A band will be identified by its mean wave number. Thus, the 3040 cm^{-1} band is the band that extends from 3030 to 3050 cm^{-1}.

Figure 1 shows our initial comparison of line by line and band model transmittances in the interval from 2800 to 3400 cm^{-1}. The optical path length in this calculation is 30 km. A convenient measure of the band model error is the logarithm of the ratio of the band model transmittance $\bar{T}_B$ to the mean line by line transmittance $\bar{T}_L$*

$$E = \text{Log}_{10}(\bar{T}_B/\bar{T}_L) \tag{10}$$

This quantity is plotted in Fig. 1b. For transmittances generally in the range $\bar{T} > 0.1$, we see that the band model does quite well. However, when $\bar{T} < 0.1$ the band model can be in error by several orders of magnitude. In particular, the errors in the bands centered at 3040 and 3060 cm^{-1} are large and opposite in direction. These two are taken as representative of low transmittance bands and will be examined in detail in the remainder of this report.

The band model and line by line transmittances in the 3040 and 3060 cm^{-1} bands are plotted as a function of distance in Figs. 2a and 3a with the corresponding error curves plotted in Figs. 2b and 3b. In the 3040 cm^{-1} band, the error is less than unity, decreases to a minimum, and then begins to increase, whereas for the 3060 cm^{-1} band the error increases monotonically.

*In this report the unit of error is called an "order of magnitude." Thus, E = 2 is a two order-of-magnitude error.

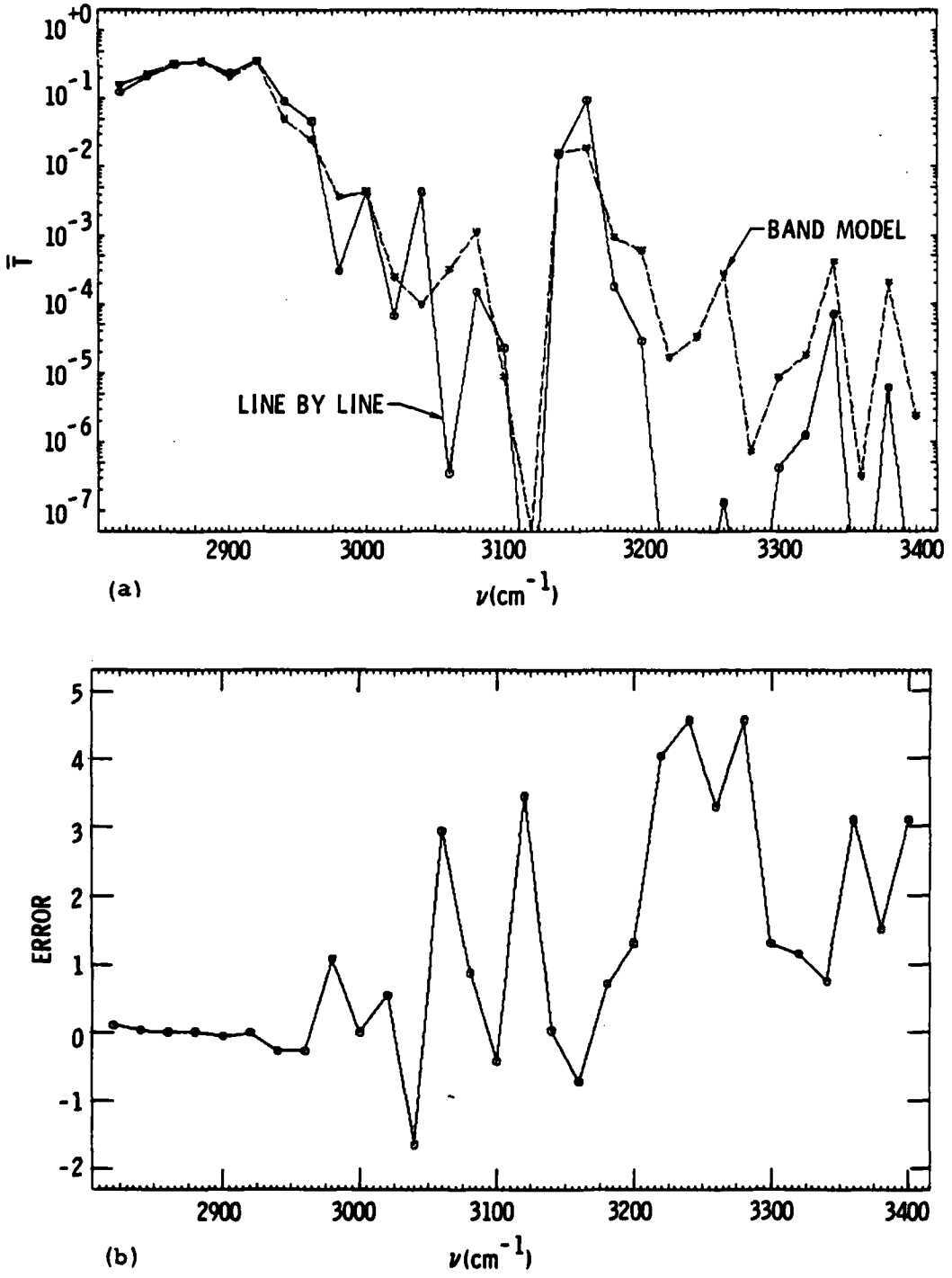

Fig. 1. Comparison of Line by Line ($\bar{T}_L$) and Band Model ($\bar{T}_B$) Transmittances at 30 km. Error = $\text{Log}_{10}(\bar{T}_B/\bar{T}_L)$.

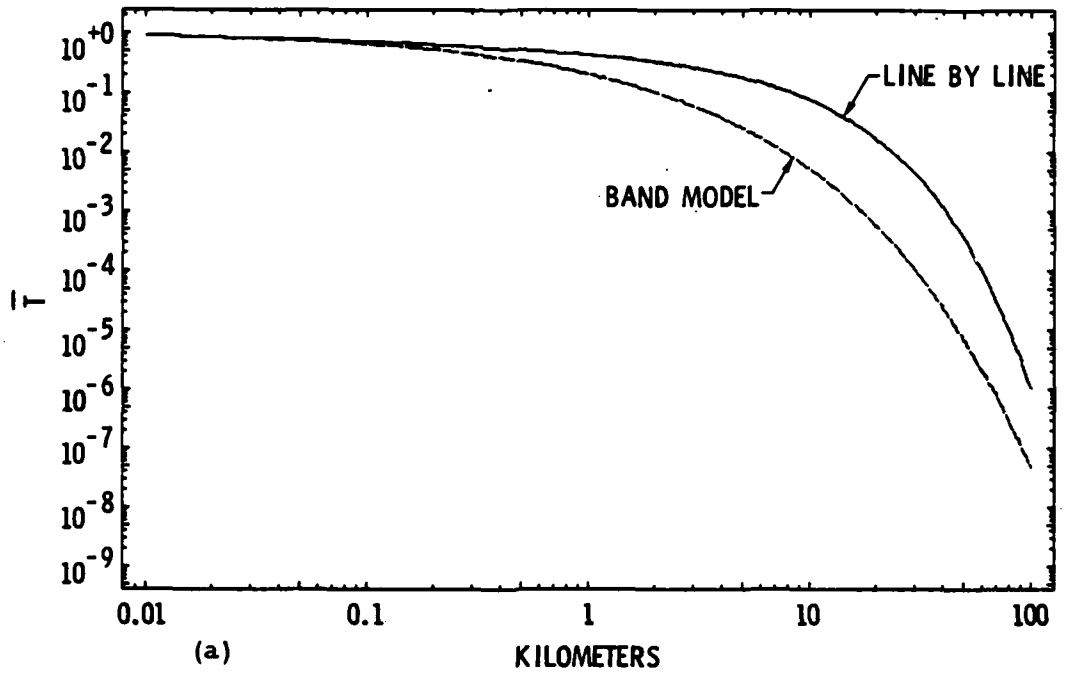

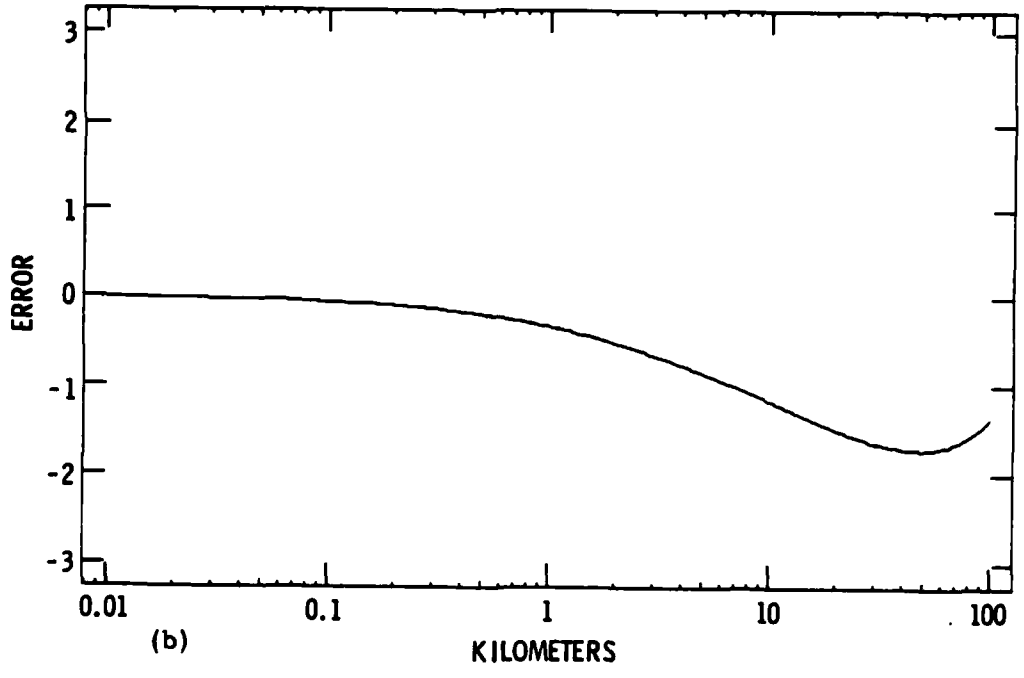

Fig. 2. Comparison of Line by Line ($\bar{T}_L$) and Band Model ($\bar{T}_B$) Transmittances for 3040 cm^{-1} Band. Error = $Log_{10}(\bar{T}_B/\bar{T}_L)$.

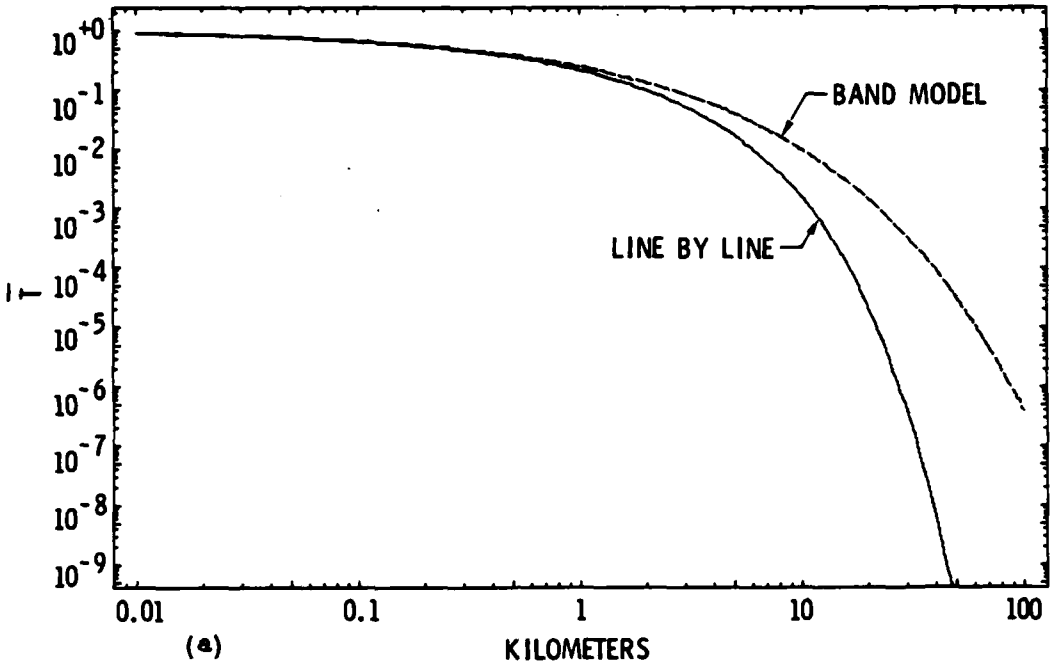

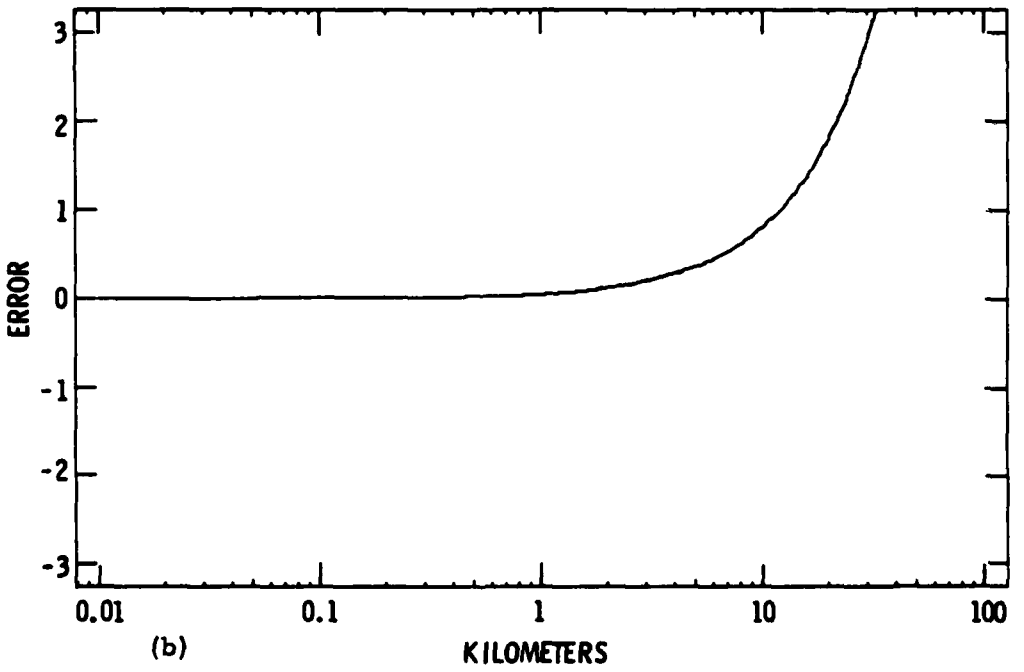

Fig. 3. Comparison of Line by Line ($\bar{T}_L$) and Band Model($\bar{T}_B$) Transmittances for 3060 cm^{-1} Band. Error $Log_{10}(\bar{T}_B/\bar{T}_L)$.

These two examples are representative of the two basic shapes for error curves. The reasons for these two basic shapes will be discussed in more detail in Section III-C.

B. H_2O LINE PARAMETER DISTRIBUTIONS

The first question that must be answered concerns the line parameter distributions. Are the line parameters actually distributed in reasonable agreement with the assumptions of statistical band theory? In order to answer this, we have plotted the distributions.

Figure 4 is a schematic plot of the lines in the two bands. The height of each line is the dimensionless strength parameter $\sigma_i = S_i/\bar{S}$ where $\bar{S}$ is the average strength for the band. In statistical band theory the lines are assumed to be randomly positioned in the band, and the line strengths are assumed to be distributed with a probability density given by the exponential-tailed inverse function.[4] This distribution function is

$$P(s) = \frac{1}{S \ln R} \left[\exp\left(\frac{-S}{S_m}\right) - \exp\left(\frac{RS}{S_m}\right)\right] \tag{11}$$

Where R and S_m are parameters, it is convenient to work with the dimensionless strength parameter $\sigma = S/\bar{S}$ (where $\bar{S}$ is the average of the distribution). The probability distribution for σ is easily shown to be

$$G(\sigma) = \bar{S}\, P(\bar{S}\, \sigma) \tag{12}$$

which evaluates to

$$G(\sigma) = \frac{1}{\sigma \ln (R)} \left[\exp(-A\sigma) - \exp(-RA\sigma)\right] \tag{13}$$

where

$$A = \bar{S}/S_m = \frac{R - 1}{R \ln R} \tag{14}$$

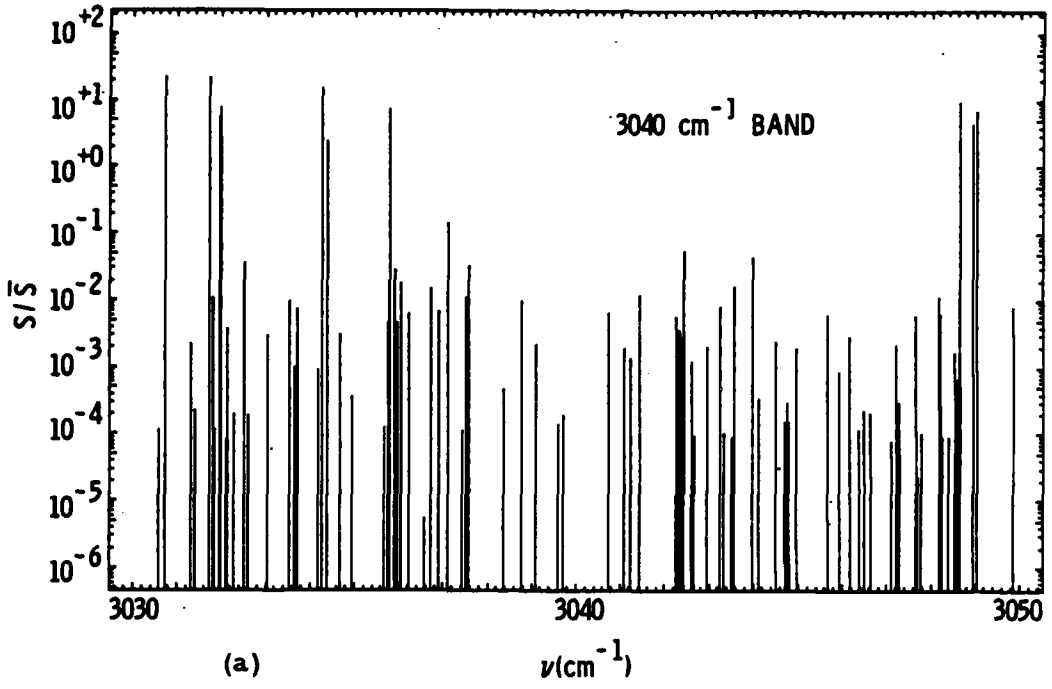

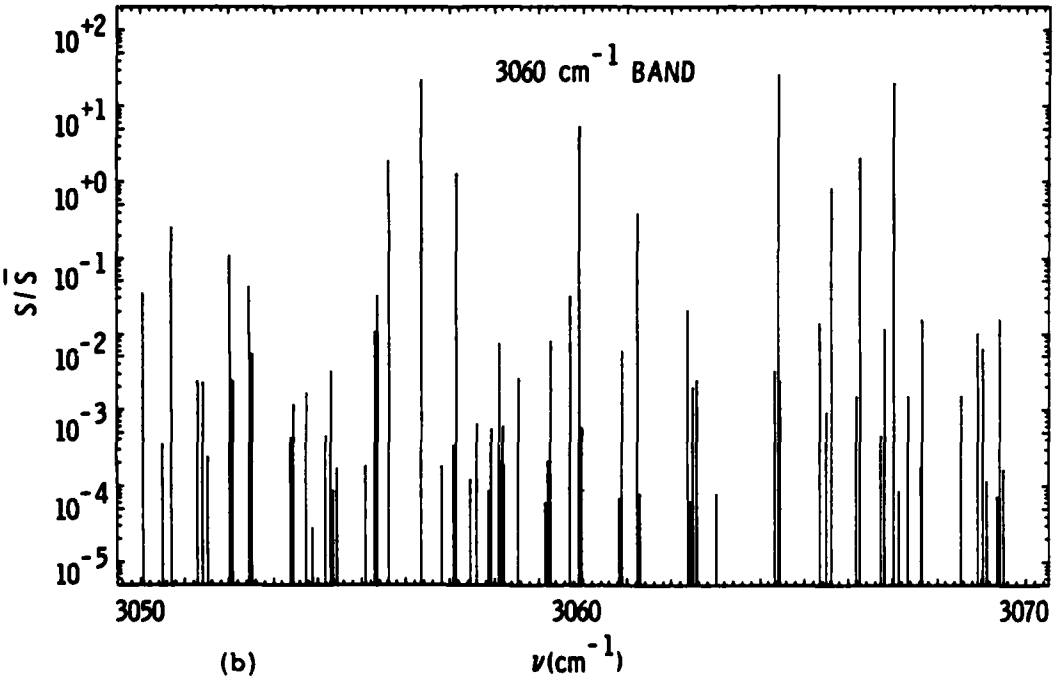

Fig. 4. Stick Diagram of H_2O Line Spectrum in the 3040 and 3060 cm^{-1} Bands.

This function is represented by the dashed curves in Fig. 5. In both graphs, $R = 10^6$. The actual density distributions of $S/\bar{S}$ in the bands are represented by the histograms in Fig. 5. The function and histograms, in each case, appear to be in reasonable agreement, vindicating the use of the exponential-tailed inverse distribution.

The line positions are assumed to be random. If this is the case, then the spacing between lines has a probability density given by

$$P(\delta) = \frac{1}{\bar{\delta}} \exp\left(-\delta/\bar{\delta}\right) \tag{15}$$

where $\bar{\delta}$ is the average value for the spacing given by

$$\bar{\delta} = \frac{\Delta\nu}{L} \tag{16}$$

The comparisons of this theoretical distribution with the actual histograms are shown in Fig. 6. Again the agreement seems reasonable.

In the band model, the line width is assumed to be a constant equal to the average value $\bar{\delta}$. The actual distributions of widths in the 3040 and 3060 cm^{-1} bands are plotted as histograms in Fig. 7. The dashed curve is a Gaussian distribution function with the same average and variance as the actual width distribution. It is obvious that the widths are not distributed normally.

Finally, the absorption coefficient $k(\nu)$, defined by Eq. (2), is plotted for our two representative bands in Fig. 8.

C. COMPUTER GENERATED LINE PARAMETERS

Additional tests of the band model were done using a set of computer generated line parameters instead of the experimental H_2O parameters obtained from the line atlas.

The computer generated line parameters are random samples drawn from infinite parent populations which are defined by their probability distribution functions. The line strength population is defined by the exponential-

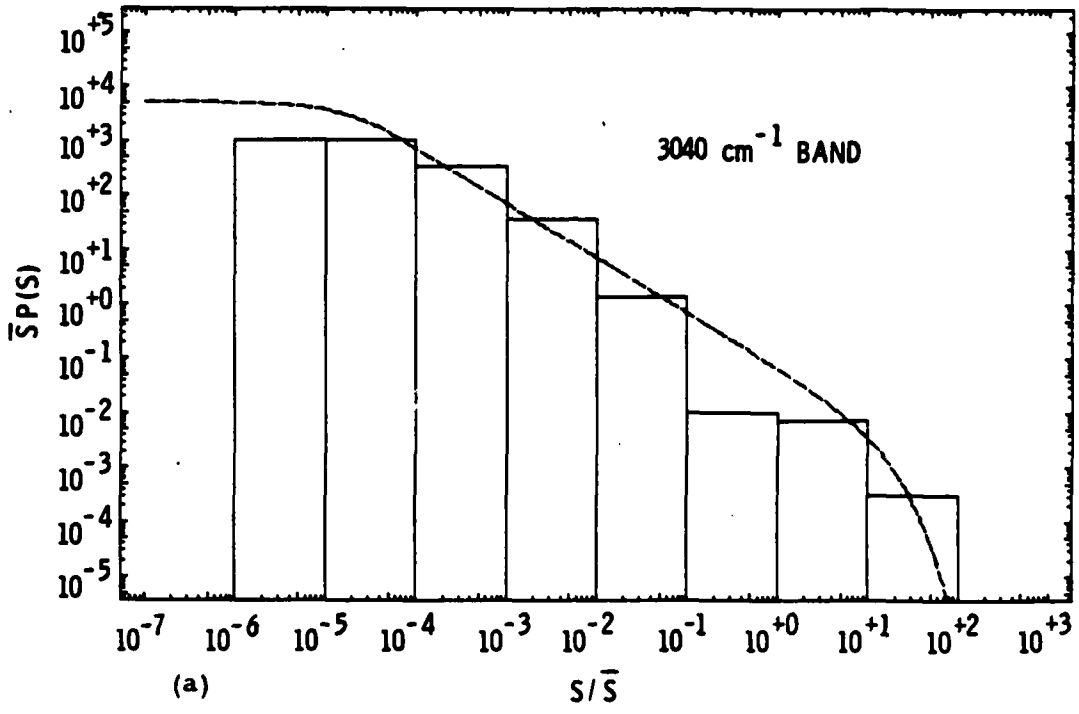

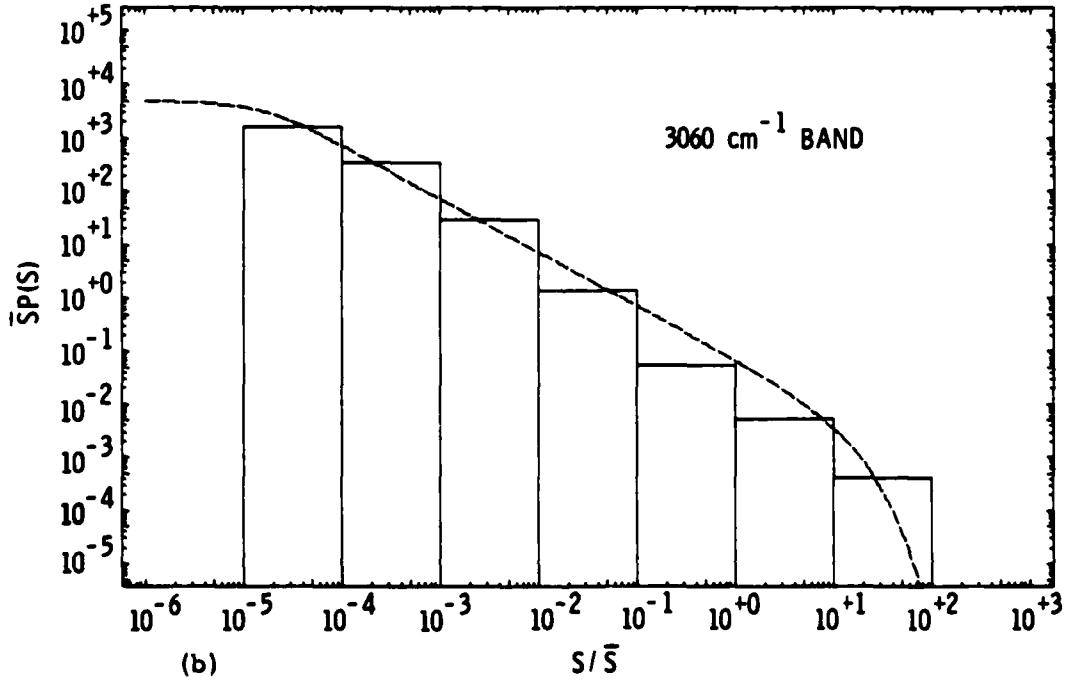

Fig. 5. Line Strength Distribution. Dashed curve is the exponential-tailed inverse function.

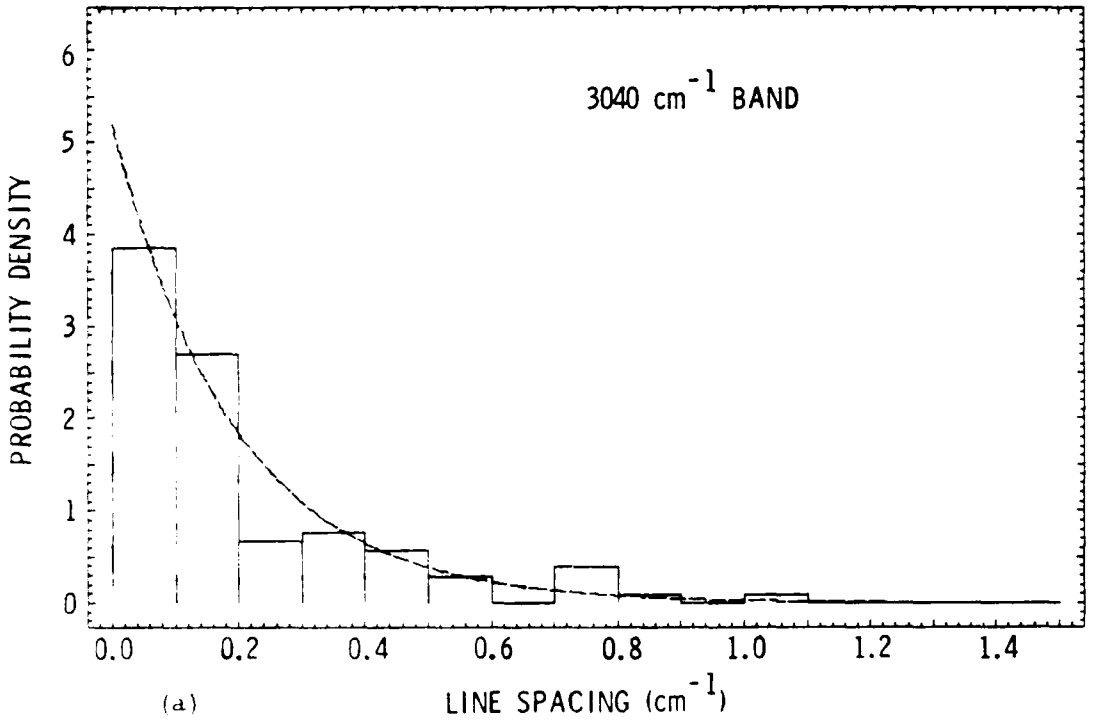

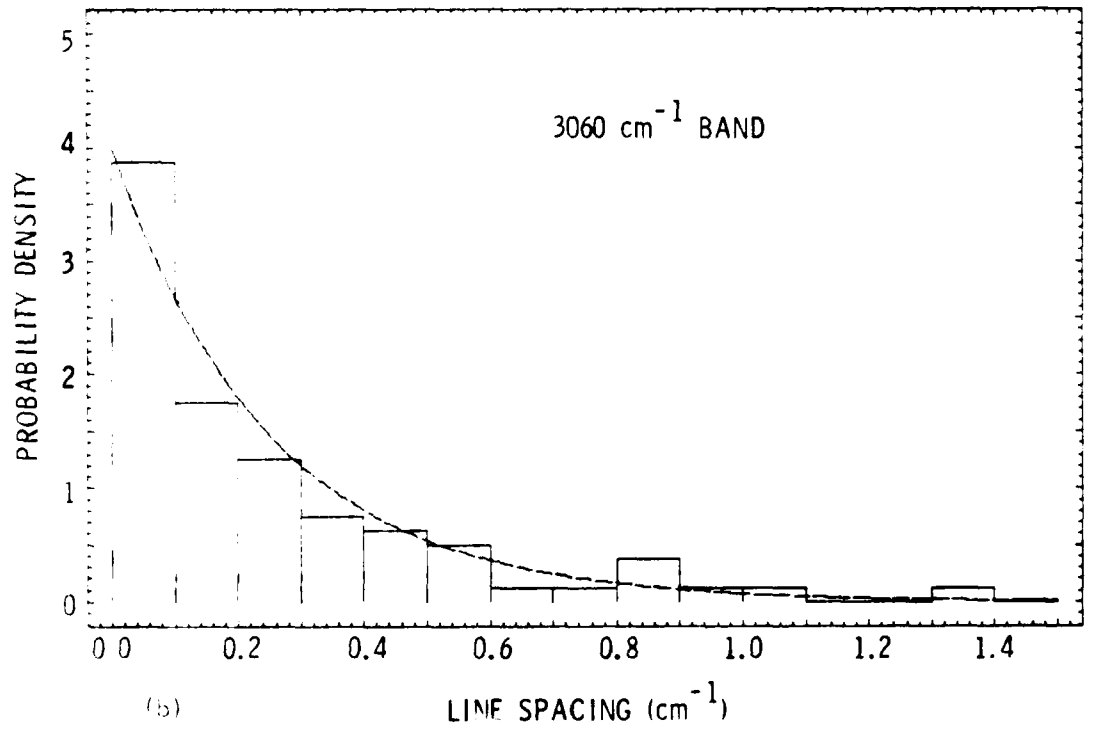

Fig. 6. Line Spacing Distribution. Dashed curve is the Poisson distribution given by Eq. (15).

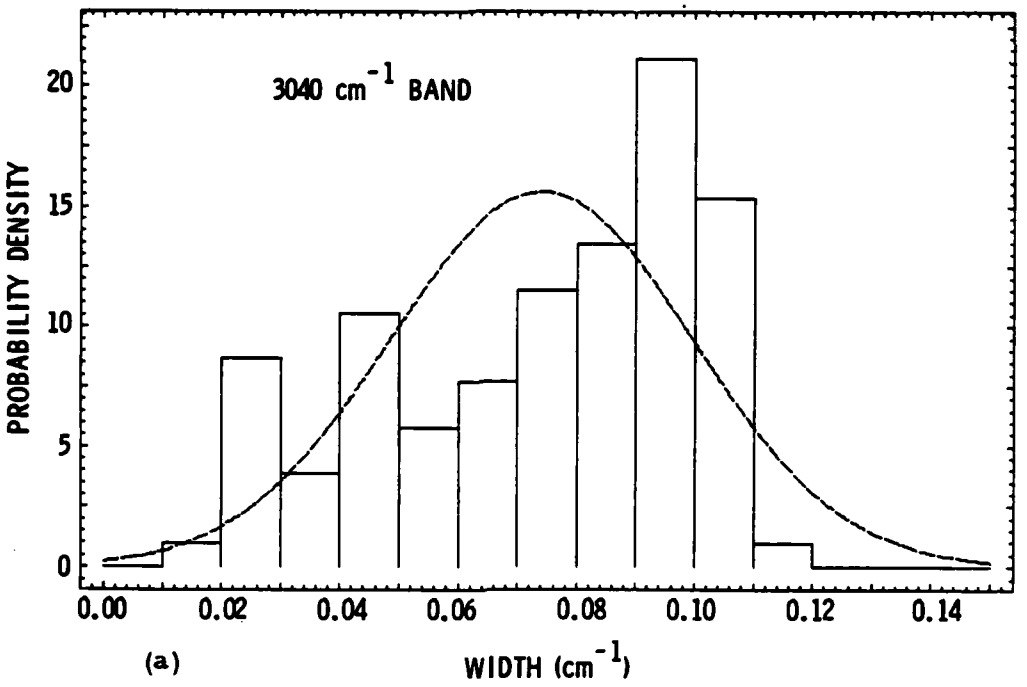

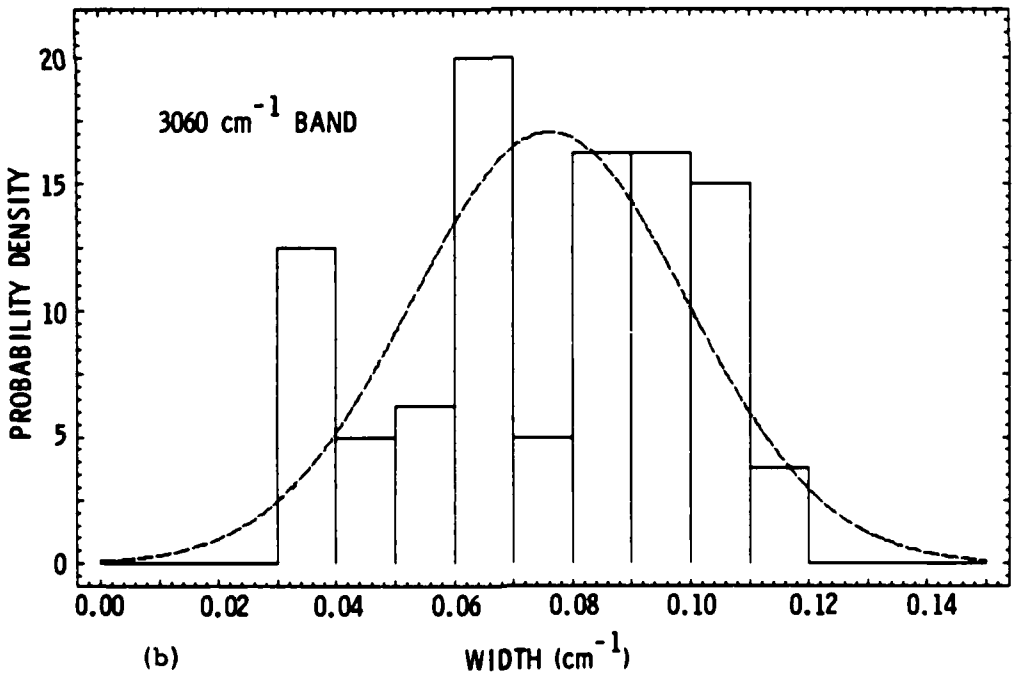

Fig. 7. Line Width Distribution. The dashed curve is a Gaussian with the same average and variance as the histogram.

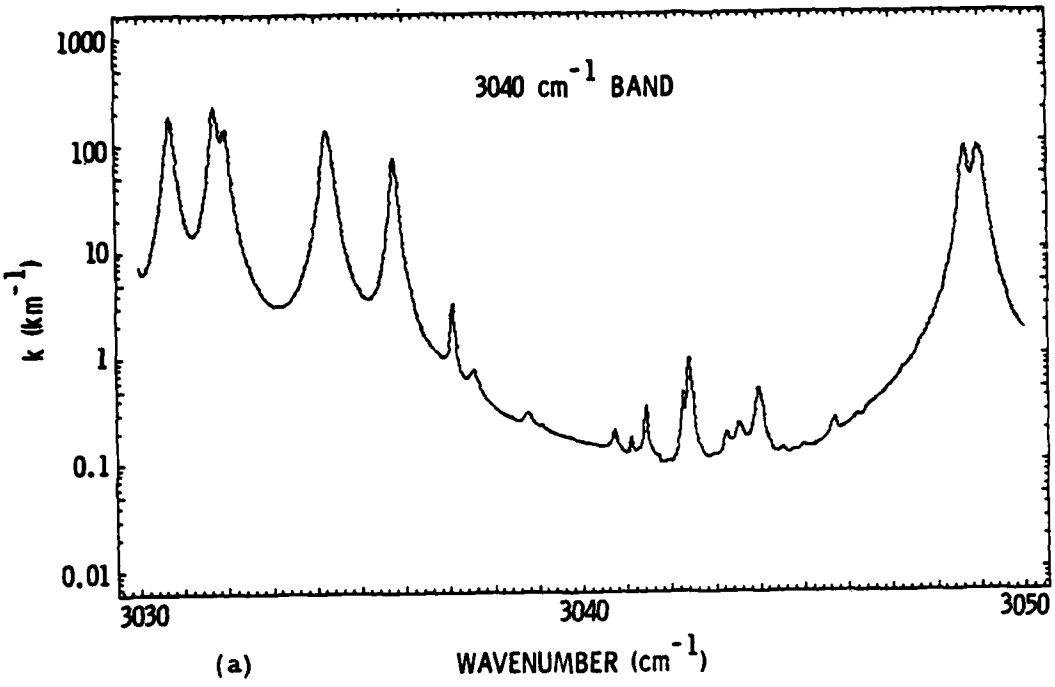

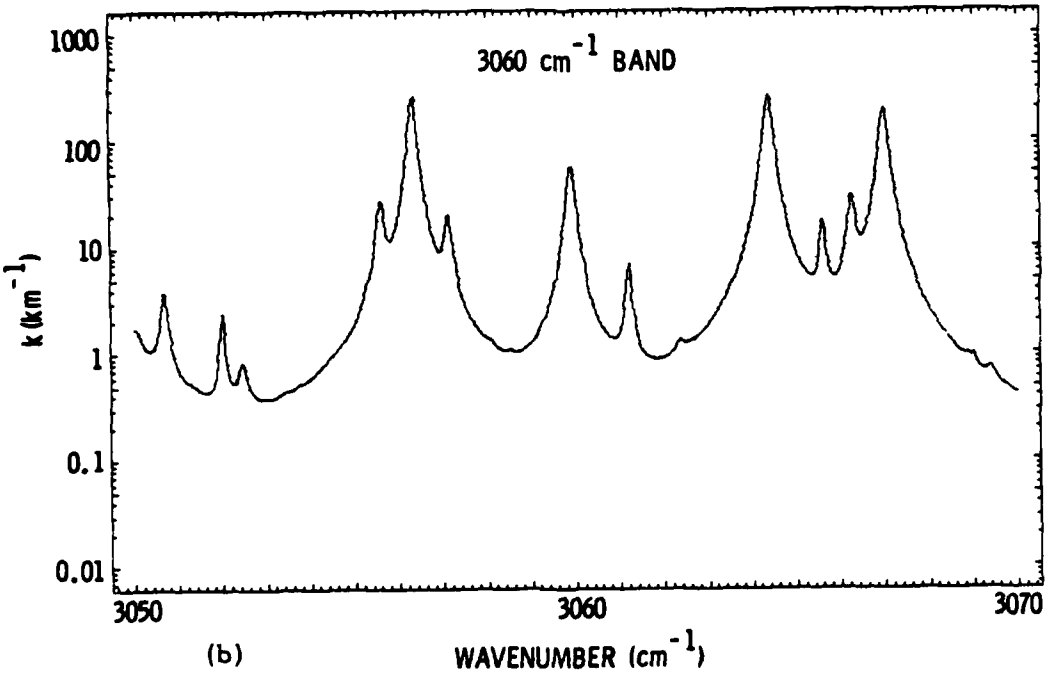

Fig. 8. Spectral Absorption Coefficient k(ν) in the 3040 and 3060 cm^{-1} Bands.

tailed inverse distribution, the line wave number population is defined to have a uniform distribution, and the line widths are all set equal to a constant.

By using these computer generated line parameters we refine our analysis of the band model error since we are now assured, as much as possible, that the line parameter distributions are in agreement with the theoretical assumptions. In addition, we can study the effect of random fluctuations on the error by generating many sets of line parameters and calculating the error curve for each.

A spectrum of 250 lines in the wave number range 0 to 50 cm^{-1} were generated. The mean transmittances were computed for the 20 cm^{-1} wide band extending from 15 to 35 cm^{-1}. The wave numbers for the lines were computed using the simple formula

$$\nu_i = 50 \cdot X_i \tag{17}$$

where the X_i are random numbers distributed uniformly in the interval 0 to 1. This array of wave numbers was then rearranged so that they were in monotonically increasing order with respect to the index i.

The line width was set equal to a constant value,

$$\delta_i = 0.075 \tag{18}$$

This constant is approximately the same as the average line width in the two H_2O bands considered previously (see Fig. 7).

The procedure for generating line strengths is more involved. The relation between the random variable X which is uniformly distributed in the range 0 to 1, and the relative line strength distribution given by Eq. (13) is

$$X = \int_0^{\sigma} G(\sigma')\, d\sigma' = H(\sigma) \tag{19}$$

Then inverting this equation and using $\sigma_i = S_i/\bar{S}$ we obtain

$$S_i = \bar{S}\, H^{-1}\,(X_i) \tag{20}$$

where the X_i are random numbers, which are independent of the random numbers used to generate the wave numbers, and H^{-1} is the inverse function of H. The functions H and H^{-1} must be computed numerically. The line strengths computed this way will have an exponential-tailed inverse distribution with an average value $\bar{S}$. (Although $\bar{S}$ is the average value for the parent population, the average line strength of the finite random sample that we will compute will deviate from this value.)

A different set of line parameters will be generated each time this process is carried out, since different random numbers are used in each run. Repeating the calculation many times will generate an ensemble of line parameter sets. (Each set is a random sample drawn from the same parent population.) Line by line and band model calculations were carried out using these computer generated line parameters. The results of a typical calculation are shown in Figs. 9 through 13. These calculations were then repeated 20 times, using different random sample line parameters in each calculation. The 20 error curves are all plotted on the same graph in Fig. 14.

The error seems to be composed of two parts, a random fluctuating component and systematic component. The random component dominates at intermediate distances and shows no bias, i.e., it is just as likely positive or negative. The systematic component dominates at large distances and increases without limit as the distance increases. This just means that, in this limit, the band model always predicts larger transmittances than the line by line calculation. Such behavior is easily understood by examining the asymptotic behavior of the band model and line by line transmittances. The asymptotic form for the band transmittance, obtained from Eq. (5), is

$$\bar{T}(x) \to \exp\left[-2\left(\frac{\bar{\gamma}\,\bar{k}}{\delta_e}\, x\right)^{1/2}\right] \tag{21}$$

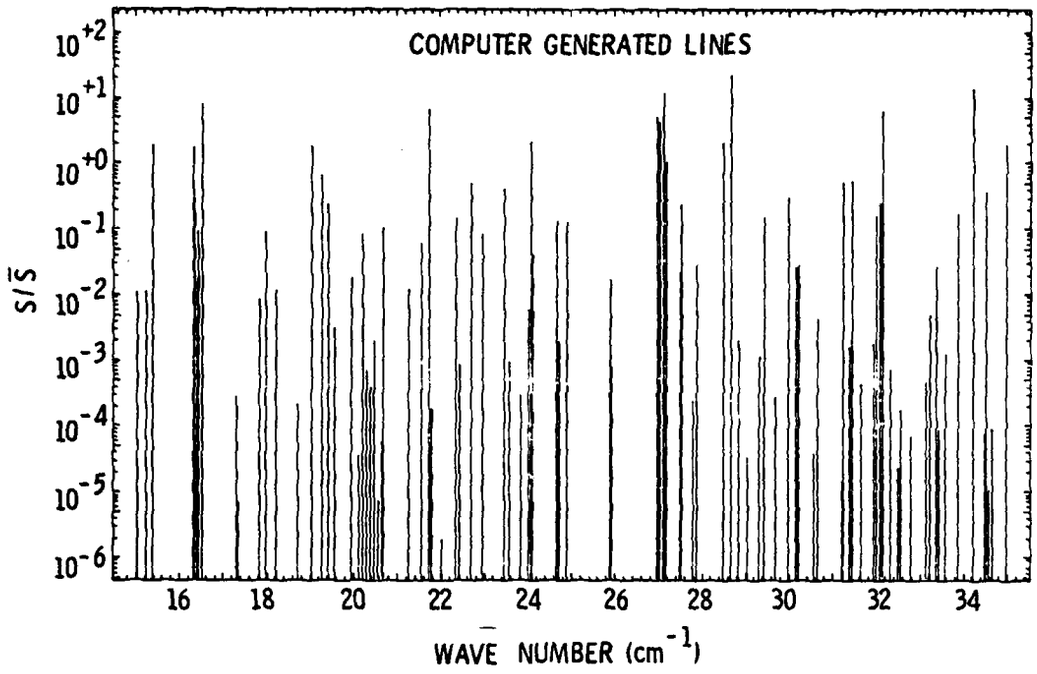

Fig. 9. Stick Diagram of a Computer Generated Line Spectrum.

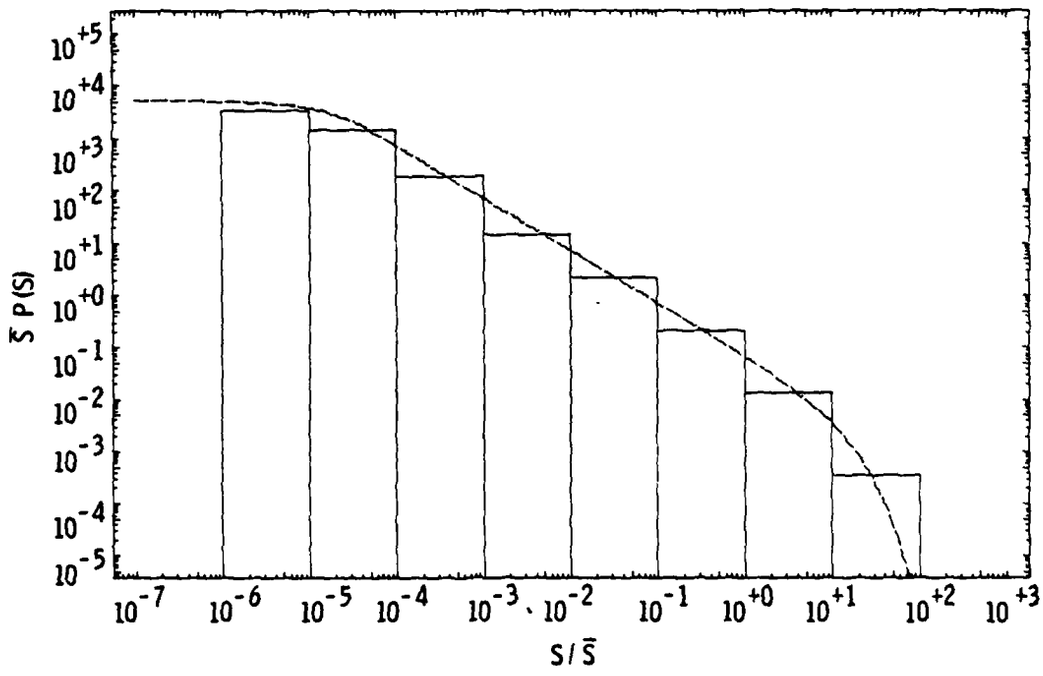

Fig. 10. Line Strength Distribution for the Computer Generated Lines. Compare with Fig. 5.

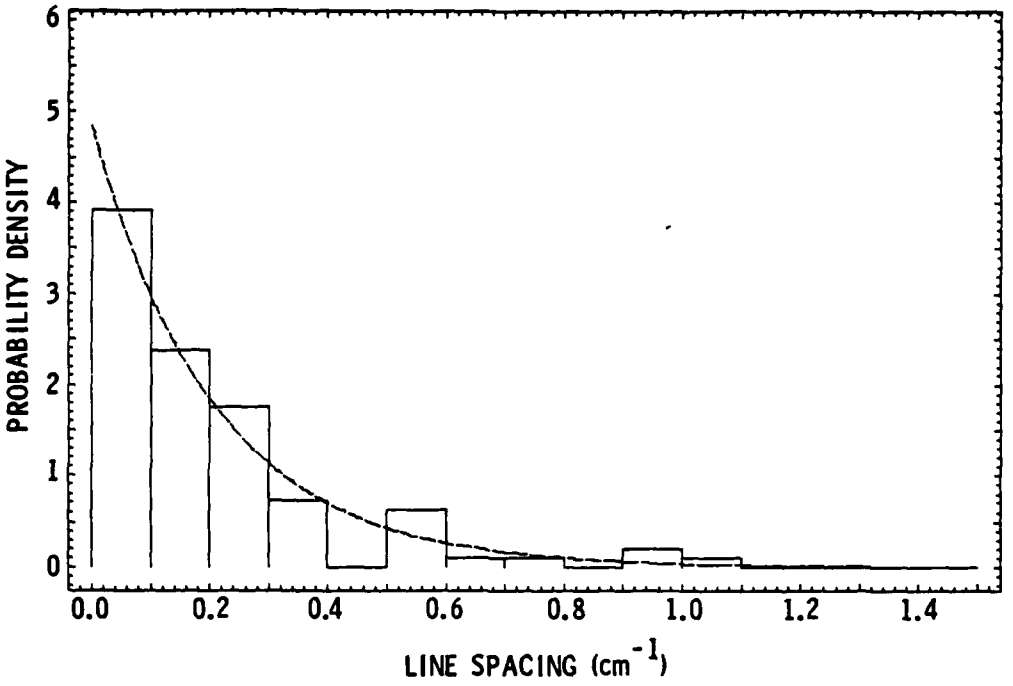

Fig. 11. Line Spacing Distribution for the Computer Generated Lines. Compare with Fig. 6.

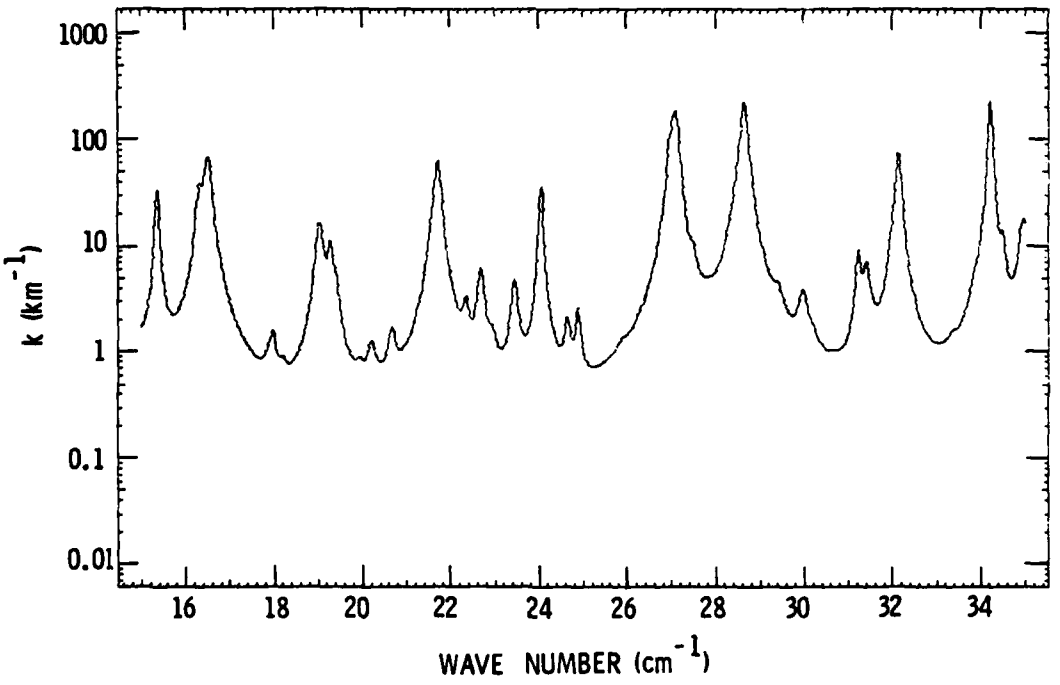

Fig. 12. Spectral Absorption Coefficient k(ν), Obtained from the Computer Generated Lines.

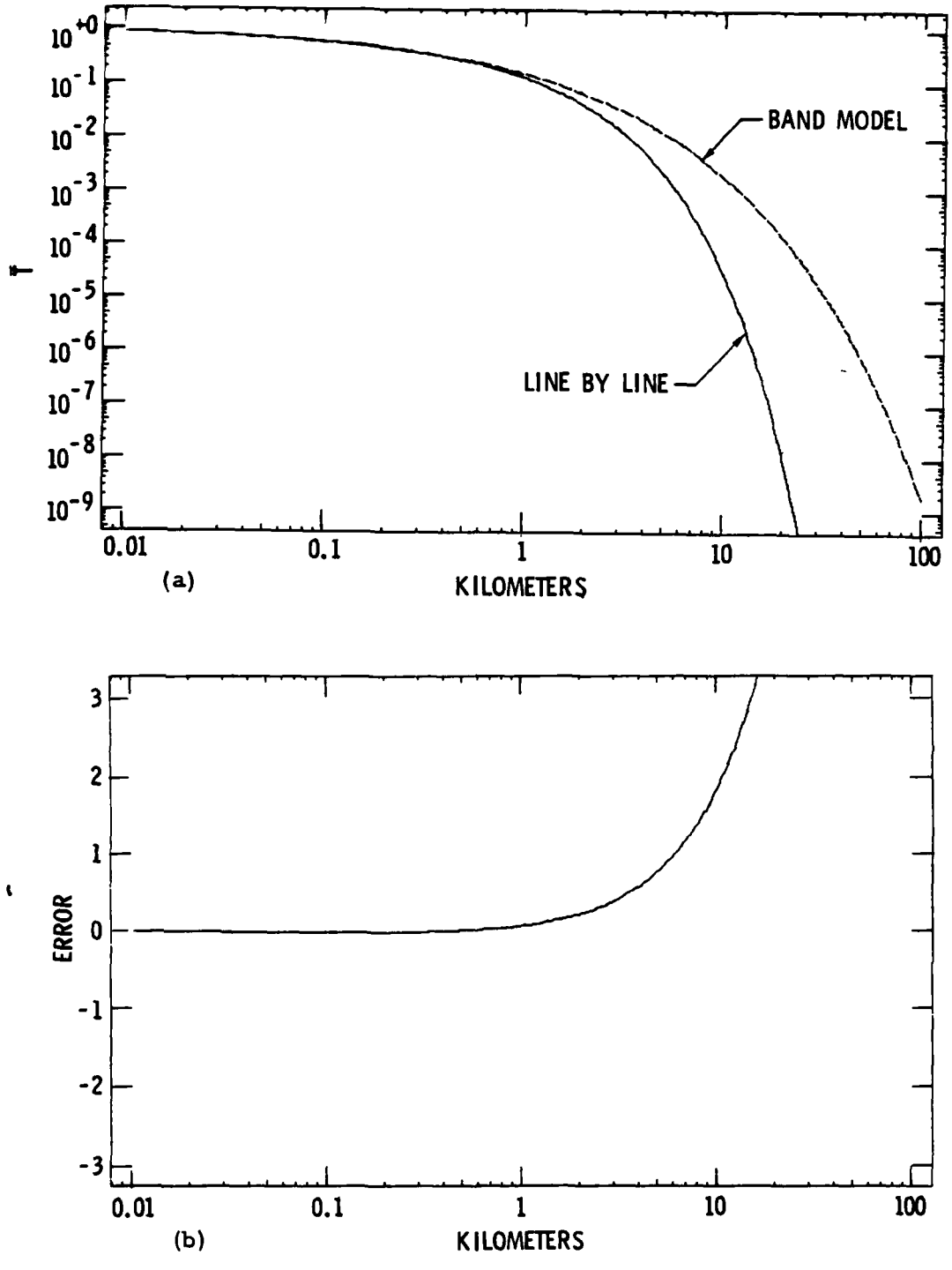

Fig. 13. Comparison of Line by Line ($\bar{T}_L$) and Band Model ($\bar{T}_B$) Transmittances Obtained from Computer Generated Lines. Error = $\text{Log}_{10}(\bar{T}_B/\bar{T}_L)$

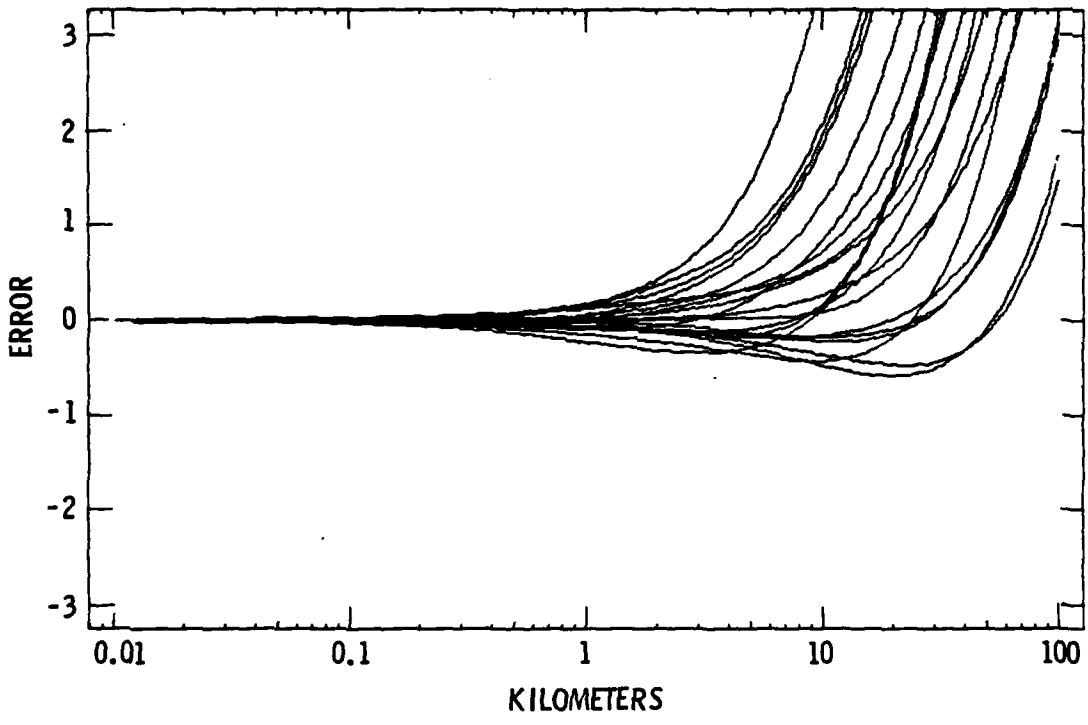

Fig. 14. Ensemble of 20 Band Model Error Curves from 20 Random Samples of Computer Generated Line Parameters.

The line by line band transmittance is given by Eq. (4). It is obvious that when x is very large only the values of $k(\nu)$ in the vicinity of the minimum value k_{min} will contribute to the integral. The integral can be evaluated by the steepest descent method to obtain the asymptotic formula

$$\overline{T} \rightarrow \left(\frac{2\pi}{k''x}\right)^{1/2} \exp(-k_{min}\, x) \tag{22}$$

where k" is the second derivative of $k(\nu)$ evaluated at the minimum. The asymptotic form of the error E is then derived from Eq. (10),

$$E \rightarrow 0.434\, [k_{min}\, x] \tag{23}$$

The essentially linear increase at large distances is evident in all the error curves plotted in Fig. 14.

The random component of the error will be discussed in Section III-C.

III. NEW TRANSMITTANCE APPROXIMATIONS

The basic result of statistical band model theory is the formula, Eq. (5), for computing the mean band transmittance. This formula has three adjustable band model parameters, which are determined either by fitting to experimental data or by calculating directly from line parameter data using Eqs. (6) through (8). The failure of this method for moderate to long optical path distances has been demonstrated in the previous section. In this section we derive alternative parameterized formulas for computing $\overline{T}(x)$ which are accurate for all values of the optical path length.

Rewrite the integral in Eq. (4) as a simple numerical quadrature

$$\overline{T}(x) = \frac{1}{\Delta\nu} \sum_{i=1}^{N} \exp[-k(\nu_i)x]\ \delta\nu \tag{24}$$

where N is the number of quadrature points, $\delta\nu$ is the spacing between points, and $\Delta\nu$ is the bandwidth. Since $\Delta\nu = N\delta\nu$, this can also be written

$$\overline{T}(x) = \frac{1}{N} \sum_{i=1}^{N} \exp[-k(\nu_i)\ x] \tag{25}$$

N must be large enough to ensure adequate accuracy. (For the calculations in the previous section we used N=1000.) The numerical ordering of the terms in the sum does not matter.* Thus the array $k(\nu_i)$ of discrete k values can be rearranged in monotonically increasing order. The points were originally spaced $\delta\nu = \Delta\nu/N$ units apart. The rearranged points are spaced $\delta p = 1/N$ units apart in the unit interval $0 \leq p \leq 1$. It is useful to regard these points as defining a monotonically increasing continuous function of p in this interval. (One could define this function, for example, by connecting the

*The basic idea of reordering k values is quite old. Application of the method and references to its previous use are given in Ref. 5.

[5]A. Arking and K. Grossman, J. Atmos. Sci. 29, 937 (1972).

points with straight line segments.) We call this function k(p) the "monotonic absorption function." The formula for the transmittance can be expressed in terms of k(p)

$$\overline{T}(x) = \int_0^1 \exp[-k(p)\, x]\, d\rho \tag{26}$$

or, in discrete form

$$\overline{T}(x) = \frac{1}{N} \sum_{i=1}^{N} \exp(-k(p_i)x] \tag{27}$$

The function k(p) is shown for the 3040 and 3060 cm^{-1} bands of H_2O in Fig. 15. These should be compared to Fig. 8 where the absorption coefficients are shown plotted as k(ν) in their natural order. It is obvious that the k(ν) functions cannot be approximated by any simple analytic function. The monotonic functions k(p) however may be amenable to simple analytic approximations. Both of the graphs of k(p), shown in semi-log plots in Fig. 15, appear to be roughly linear. Therefore the first approximation we will try is just a simple exponential function

$$k(p) \approx k_0 \exp(bp) \tag{28}$$

A. TWO-PARAMETER APPROXIMATION

In the previous section it was shown that the long range behavior of $\overline{T}(x)$ is dominated by k_{min}. Since we want the long range behavior to be correct, we define $k_0 = k_{min} = k(0)$. At the other extreme, the very short range behavior of $\overline{T}(x)$ is determined by the average value of k. This is easily proven. For very small values of x, the exponential in Eq. (26) can be replaced by the first two terms of its power series expansion, thus

$$\overline{T}(x) \approx 1 - \langle k \rangle\, x \tag{29}$$

points with straight line segments.) We call this function k(p) the "monotonic absorption function." The formula for the transmittance can be expressed in terms of k(p)

$$\bar{T}(x) = \int_0^1 \exp[-k(p)\, x]\, d\rho \tag{26}$$

or, in discrete form

$$\bar{T}(x) = \frac{1}{N} \sum_{i=1}^{N} \exp(-k(p_i)x] \tag{27}$$

The function k(p) is shown for the 3040 and 3060 cm^{-1} bands of H_2O in Fig. 15. These should be compared to Fig. 8 where the absorption coefficients are shown plotted as $k(\nu)$ in their natural order. It is obvious that the $k(\nu)$ functions cannot be approximated by any simple analytic function. The monotonic functions k(p) however may be amenable to simple analytic approximations. Both of the graphs of k(p), shown in semi-log plots in Fig. 15, appear to be roughly linear. Therefore the first approximation we will try is just a simple exponential function

$$k(p) \approx k_0 \exp(bp) \tag{28}$$

A. TWO-PARAMETER APPROXIMATION

In the previous section it was shown that the long range behavior of $\bar{T}(x)$ is dominated by k_{min}. Since we want the long range behavior to be correct, we define $k_0 = k_{min} = k(0)$. At the other extreme, the very short range behavior of $\bar{T}(x)$ is determined by the average value of k. This is easily proven. For very small values of x, the exponential in Eq. (26) can be replaced by the first two terms of its power series expansion, thus

$$\bar{T}(x) \approx 1 - \langle k \rangle\, x \tag{29}$$

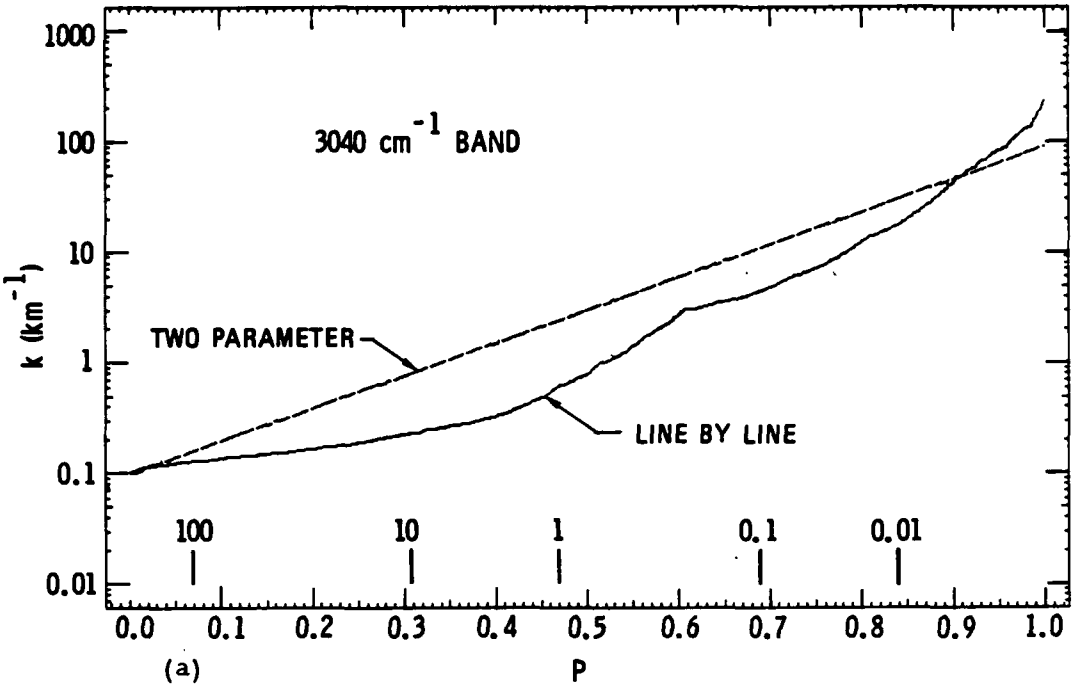

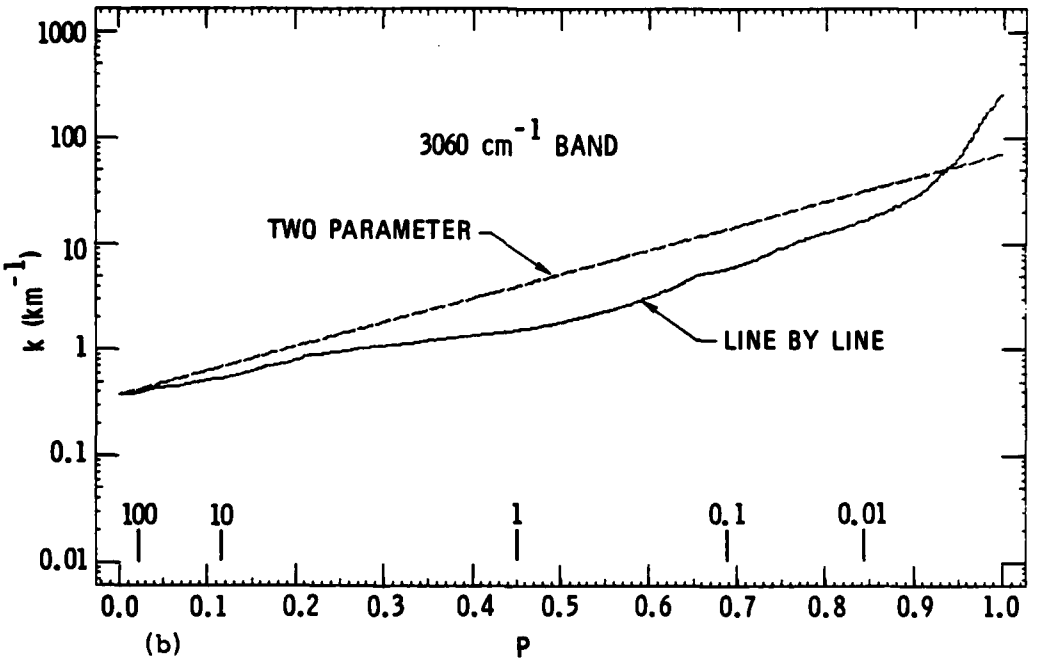

Fig. 15. Monotonic Absorption Function k(p). Comparison of line by line and two-parameter model. Tick marks are upper integration limits used in Eq. (26) for 90% accuracy at distances indicated in kilometers.

where

$$\langle k \rangle = \int_0^1 k(p)\, dp \tag{30}$$

is the average value of k.

The parameter b in Eq. (28) is chosen so that the average value of the exponential approximation is equal to $\langle k \rangle$. Thus, we obtain

$$\langle k \rangle = k_0 \int_0^1 \exp(bp)\, dp \tag{31}$$

or

$$\frac{\langle k \rangle}{k_0} = \frac{e^b - 1}{b} \tag{32}$$

which can be solved numerically for b. Using these values for the parameters k_0 and b, the exponential approximation to k(p) is plotted as the dashed straight lines in Fig. 15. The approximate transmittance is then computed by substituting the function k(p) given by Eq. (28) into Eq. (26) and integrating the resulting expression. The integral can be evaluated analytically.

To accomplish this, the variable of integration in Eq. (26) is changed from p to k

$$\overline{T}(x) = \int_{k_0}^{k_1} \exp[kx]\, f(k)\, dk \tag{33}$$

where the function f(k) is

$$f(k) = \frac{dp(k)}{dk} \tag{34}$$

and

$$k_1 = k_0 \exp(b) \tag{35}$$

[The meaning of the function f(k) will be discussed in more detail later.]

Equation (28) is easily inverted to obtain

$$p(k) = \frac{1}{b} \ln(k/k_0) \tag{36}$$

and therefore, using Eq. (34)

$$f(k) = \frac{1}{bk} \tag{37}$$

Substituting this expression into Eq. (33) gives

$$\overline{T}(x) = \frac{1}{b} [E_1 (k_0 x) - E_1 (k_1 x)] \tag{38}$$

where $E_1(x)$ is the exponential-integral function defined by[6]

$$E_1(x) = \int_x^\infty \frac{e^{-t}}{t} dt \tag{39}$$

Very efficient methods are available for the numerical evaluation of the exponential integral function.[6] The function, Eq. (38), has three parameters k_0, k_1, and b. However only two are independent. Using Eq. (35) we express b in terms of k_0 and k_1 obtaining our final two-parameter expression for $\overline{T}(x)$

$$\overline{T}(x) = \frac{1}{\ln(k_1/k_0)} [E_1(k_0 x) - E_1(k_1 x)] \tag{40}$$

This function was evaluated numerically and the approximate mean transmittance curves are shown plotted in Figs. 16a and 17a along with the precise line by line results for comparison. Below these graphs in Figs. 16b and 17b are the error curves for the two-parameter approximation and also, for comparison, the error curves for the band model transmittances (see Figs. 2b and 3b).

---

[6] M. Abramowitz and I. Stegun, Handbook of Mathematical Functions, Dover, New York (1965)

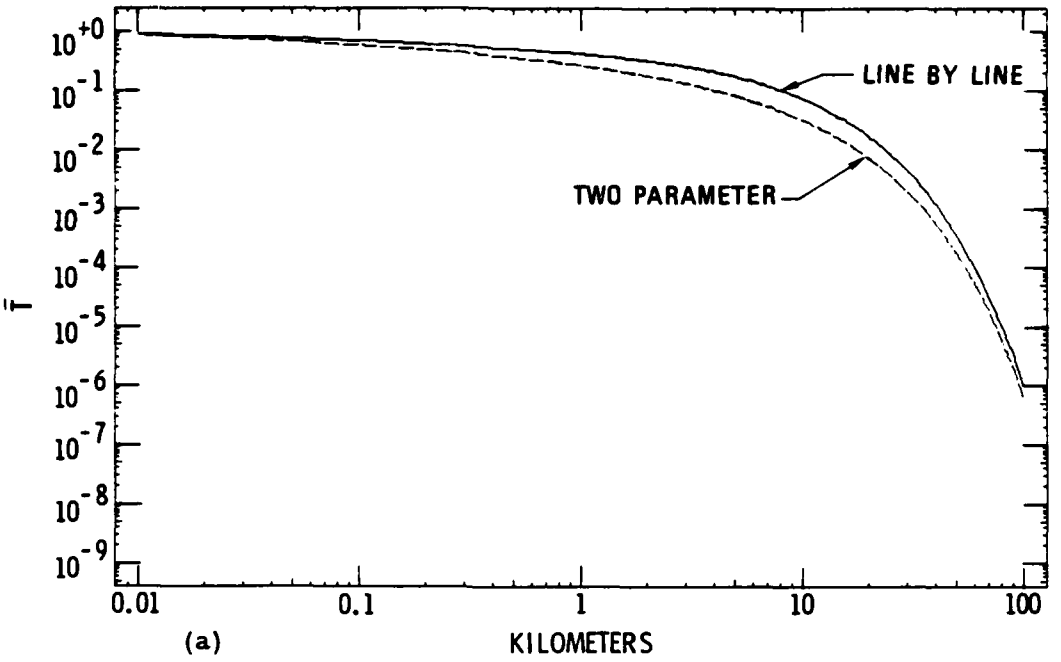

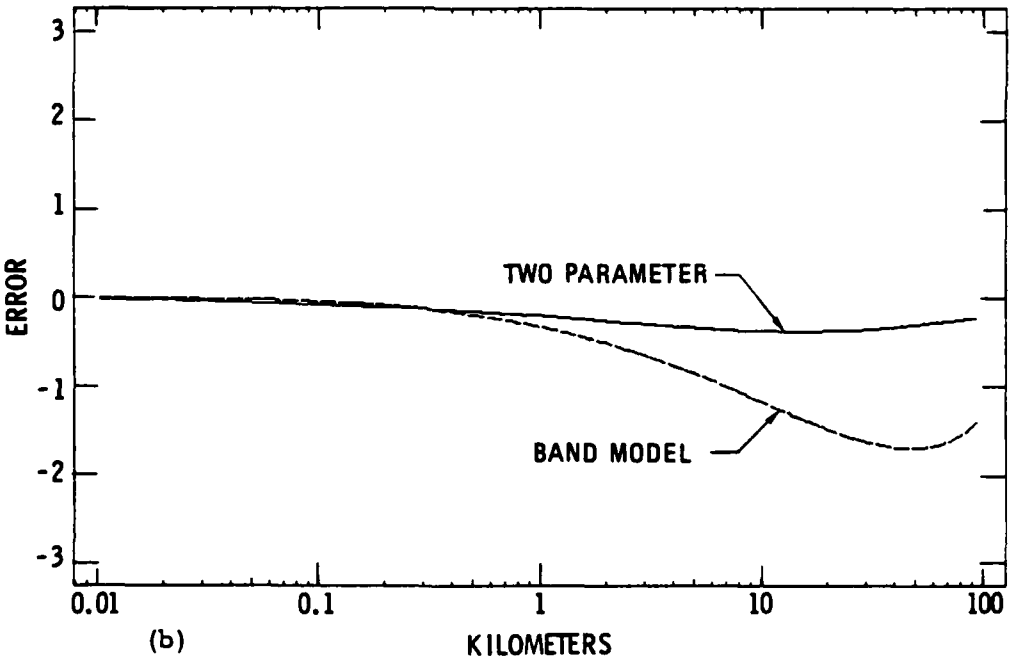

Fig. 16. Comparison of Line by Line ($\bar{T}_L$) and Two-Parameter Model ($\bar{T}_2$) Transmittances for 3040 cm^{-1} Band. Error = $Log_{10}(\bar{T}_2/\bar{T}_L)$. The band model error is also shown for comparison.

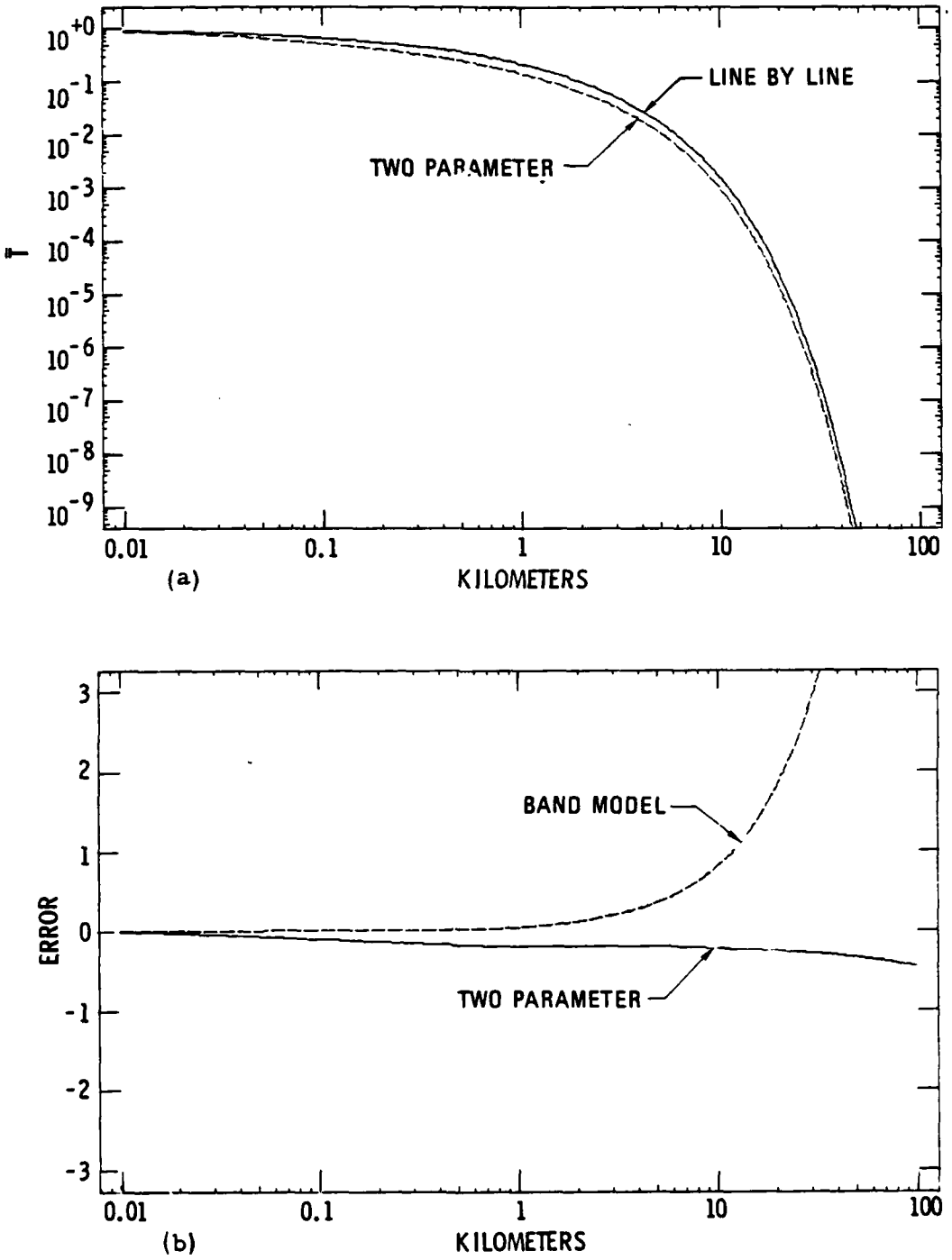

Fig. 17. Comparison of Line by Line ($\bar{T}_L$) and Two-Parameter Model ($\bar{T}_2$) Transmittances for 3060 cm^{-1} Band. Error = $\text{Log}_{10}(\bar{T}_2/\bar{T}_L)$. The band model error is also shown for comparison.

The range of integration in Eq. (26) for the variable of integration p is $0 \leq p \leq 1$. For large values of the distance x, the contribution from the upper portion of this integration range is very small. In order to demonstrate this quantitatively, we have computed the upper limit of integration required to compute 90% of the value of $\overline{T}(x)$ for various fixed values of x. These upper integration limits are shown as tick marks in Fig. 15 and are labeled with the appropriate value of distance x in kilometers. We see that even for fairly small distances, the upper portion of the integration range does not make much contribution. This would suggest that any analytic fit to k(p) should be weighted to have the least error in the lower part of the p range. The present procedure for calculating the slope parameter b overemphasizes the large k values. From Fig. 15 we see that a better fit would be obtained in the lower portion of the k(p) curve if the slope parameter b were less.

A new procedure, which gives more weight to the lower k values, was tried for fitting the analytic function, Eq. (28), to k(p). The parameter k_0 is still defined to be the minimum, $k_0 = k(0)$. However, instead of computing the average value of k as in Eq. (30), we now compute the average value of the natural log of k

$$< \ell n(k) > = \int_0^1 \ell n\ [k(p)]\ dp \tag{41}$$

The parameter b is determined by requiring that the average value of the natural log of the exponential approximation, Eq. (28), is equal to $< \ell n(k) >$

$$< \ell n(k) > = \int_0^1 \ell n\ [k_0\ \exp(bp)]\ dp \tag{42}$$

This is easy to solve and we obtain

$$b = 2\ [<\ell n(k)> - \ell n(k_0)] \tag{43}$$

The new value for the parameter k_1 is then computed by substituting this value of b into Eq. (35) and the transmittance is computed using Eq. (40).

This new analytic approximation to k(p) is shown plotted as the dashed straight line in Fig. 18. The slope of the line has been reduced from that of Fig. 15 and a better fit to k(p) is obtained in the lower range of the curve. In Figs. 19 and 20, which show the transmittances and error curves for our two example bands, the error has been reduced from that shown in Figs. 16 and 17. Thus, the second method for computing b, which gives more weight to the lower k values, is slightly superior. It has a very simple graphical interpretation in the semi-log plots shown in Fig. 18. The area under the straight line approximation is equal to the area under the line by line k(p). (Unless otherwise stated, in any future reference to the two-parameter method, the parameters are computed by the $< \ell n(k) >$ method.)

B. THREE-PARAMETER APPROXIMATION

Any further significant improvement in accuracy can only be accomplished by increasing the flexibility of the analytic function used to approximate k(p). We have done this by dividing the integration range into two parts, $0 \leq p \leq 1/2$ and $1/2 \leq p \leq 1$, and approximating k(p) in each of these regions by an exponential function

$$k(p) = \begin{cases} k_0 \exp[b_1 p], & 0 \leq p \leq 1/2 \\ k_{1/2} \exp[b_2 (p-1/2)], & 1/2 \leq p \leq 1 \end{cases} \tag{44}$$

The function is required to be continuous which implies

$$k_{1/2} = k_0 \exp[b_1/2] \tag{45}$$

The maximum value of this function is

$$k_1 = k_{1/2} \exp[b_2/2] \tag{46}$$

The inverse function to Eq. (44) is

$$p(k) = \begin{cases} \frac{1}{b_1} \ell n(k/k_0) & k_0 \leq k \leq k_{1/2} \\ \frac{1}{b_2} \ell n(k/k_1) & k_{1/2} \leq k \leq k_1 \end{cases} \tag{47}$$

and therefore from Eq. (34)

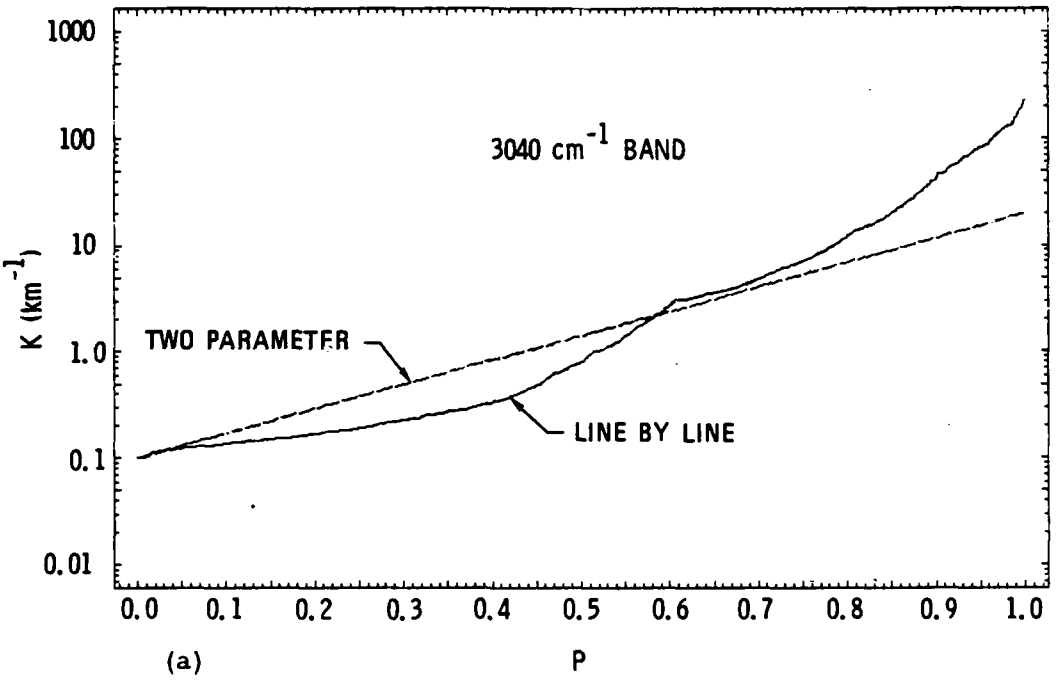

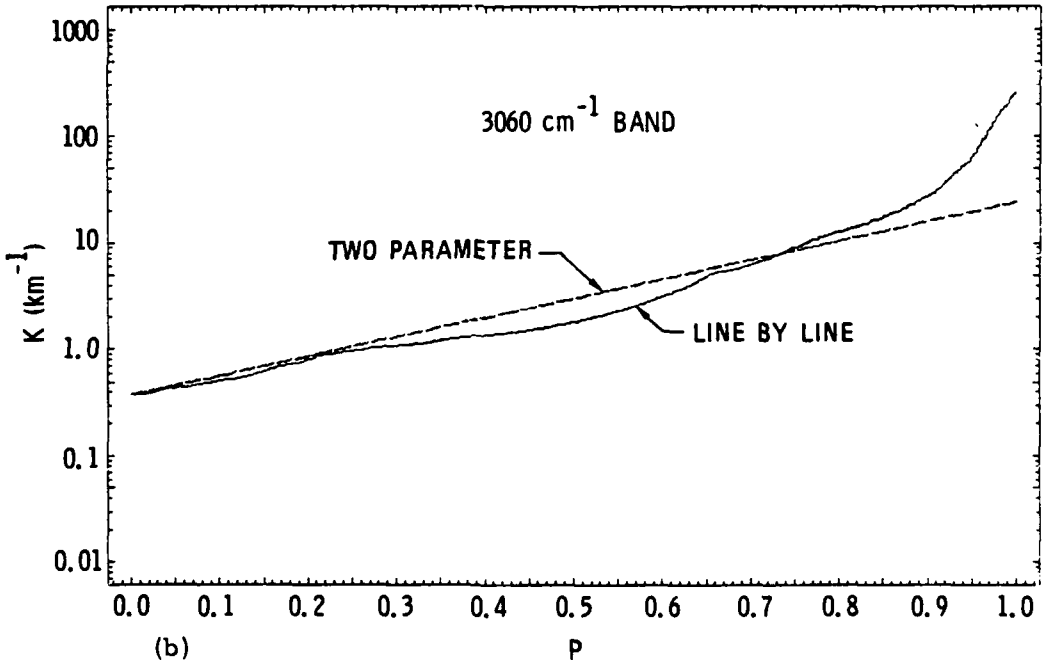

Fig. 18. Monotonic Absorption Function k(p). Same as Fig. 15 Except for Alternate Definition of Parameters in the Two-Parameter Model (see text).

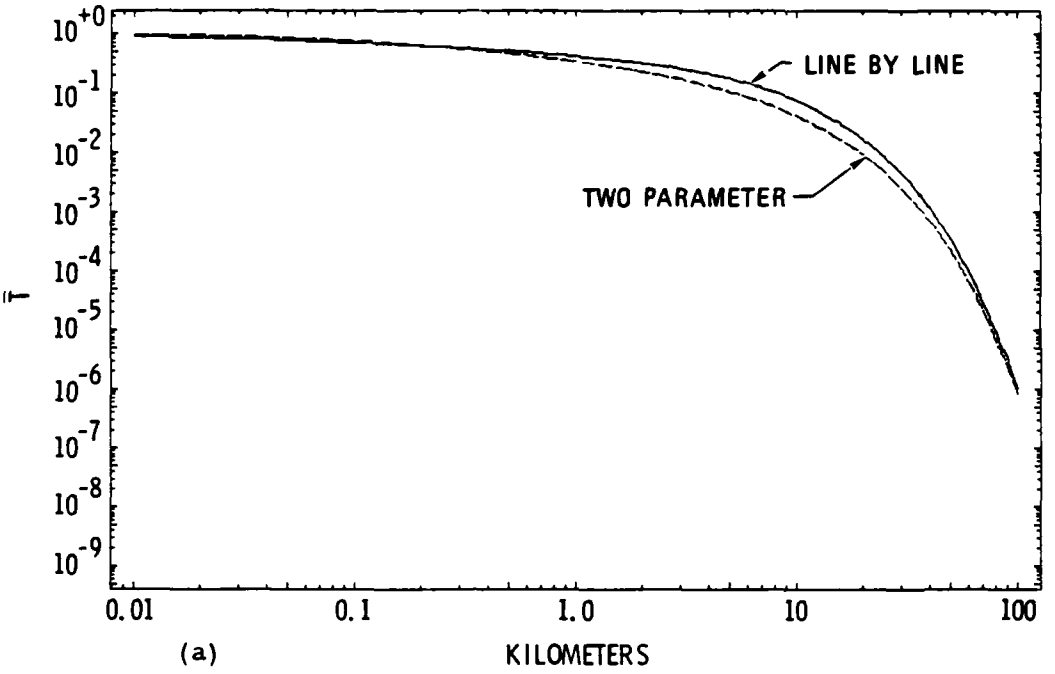

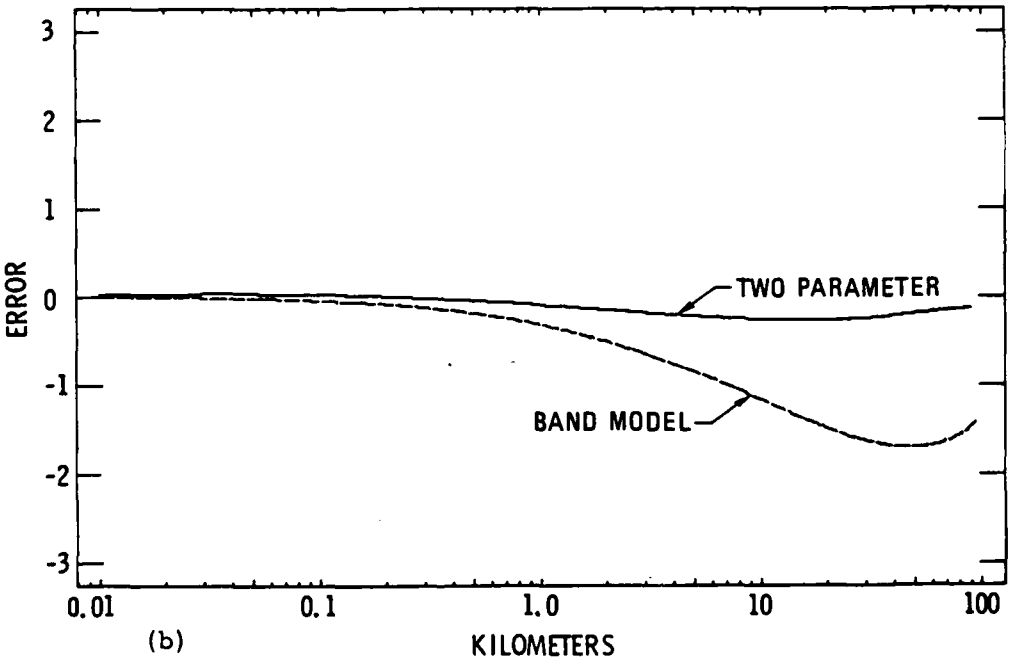

Fig. 19. Comparison of Line by Line ($\bar{T}_L$) and Alternate Two-Parameter Model ($\bar{T}_2$) Transmittances for the 3040 cm^{-1} Band. Error = $Log_{10}(\bar{T}_2/\bar{T}_L)$. The band model error is also shown for comparison.

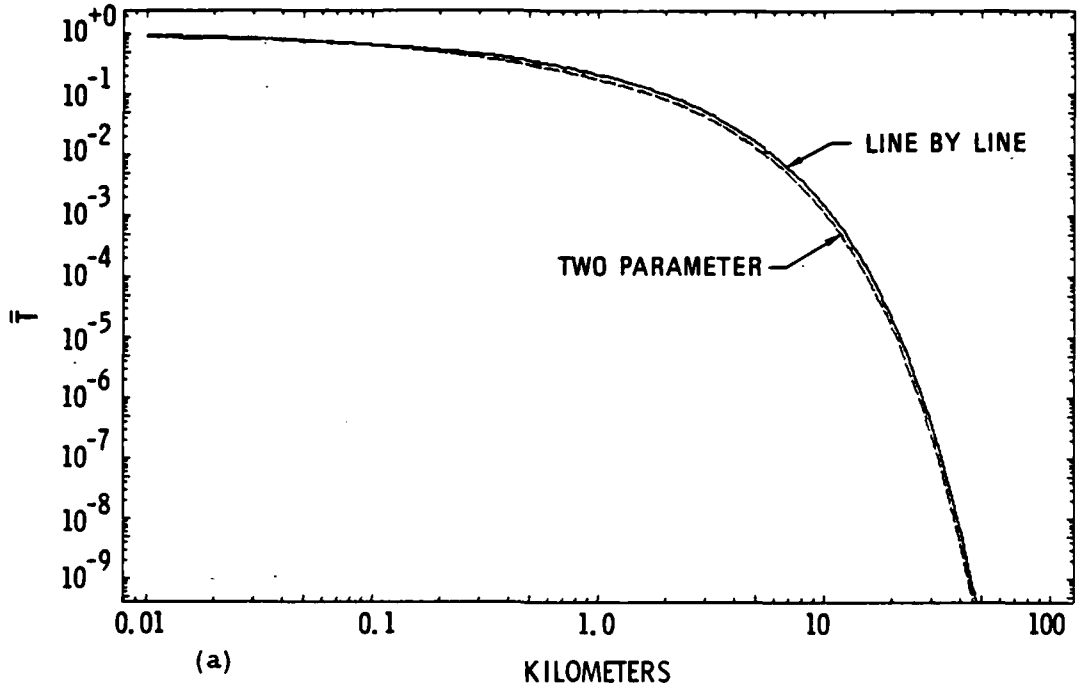

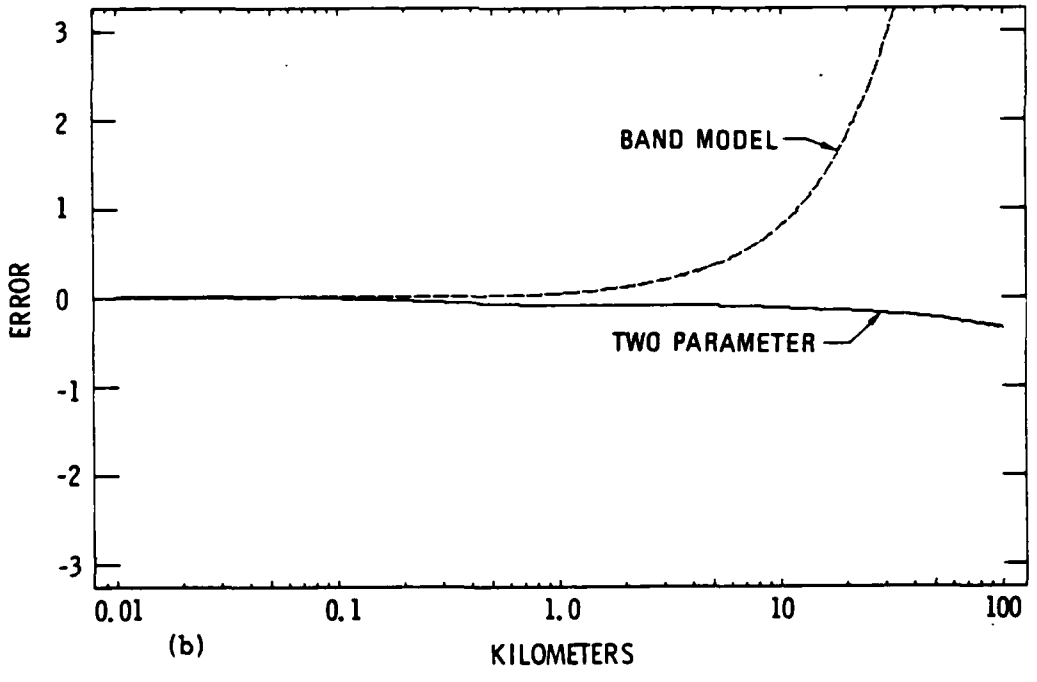

Fig. 20. Comparison of Line by Line ($\bar{T}_L$) and Alternate Two-Parameter Model ($\bar{T}_2$) Transmittances for the 3060 cm^{-1} Band. Error = $Log_{10}(\bar{T}_2/\bar{T}_L)$. Model error is also shown for comparison.

$$f(k) = \begin{cases} \dfrac{1}{b_1 k} & k_0 \leq k \leq k_{1/2} \\ \dfrac{1}{b_2 k} & k_{1/2} \leq k \leq k_1 \end{cases} \tag{48}$$

Note that $f(k)$ is discontinuous at $k = k_{1/2}$.

The minimum value of the analytic approximation is k_0. Just as in the previous cases, this is defined to be equal to the true minimum value k_{min} of $k(p)$,

$$k_0 = k_{min} = k(0) \tag{49}$$

The parameters b_1 and b_2 are defined similarly to the previous case. If we calculate the average values of $\ell n[k(p)]$ in each half region

$$\langle \ell n(k) \rangle_1 = \int_0^{1/2} \ell n[k(p)]\, dp \tag{50}$$

$$\langle \ell n(k) \rangle_2 = \int_{1/2}^{1} \ell n[k(p)]\, dp \tag{51}$$

and equate these to the values obtained when the analytic approximation, Eq. (44), is substituted for $k(p)$ in Eqs. (50) and (51),

$$b_1 = 4\,[2\,\langle \ell n(k) \rangle_1 - \ell n(k_0)] \tag{52}$$

and

$$b_2 = 4[2\,\langle \ell n(k) \rangle_2 - \ell n(k_{1/2})] \tag{53}$$

The value of $k_{1/2}$ in Eq. (53) is computed using Eq. (45). With all the parameters defined, the analytic approximation, Eq. (44), is evaluated and plotted in Fig. 21. This should be compared with the previous two-parameter approximation in Fig. 18.

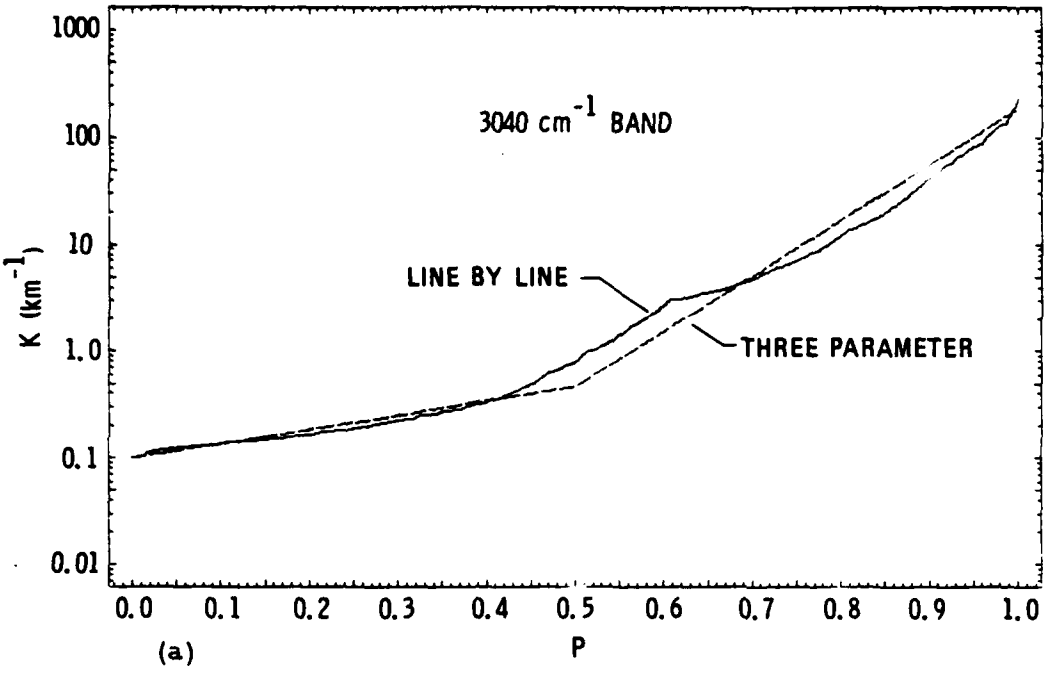

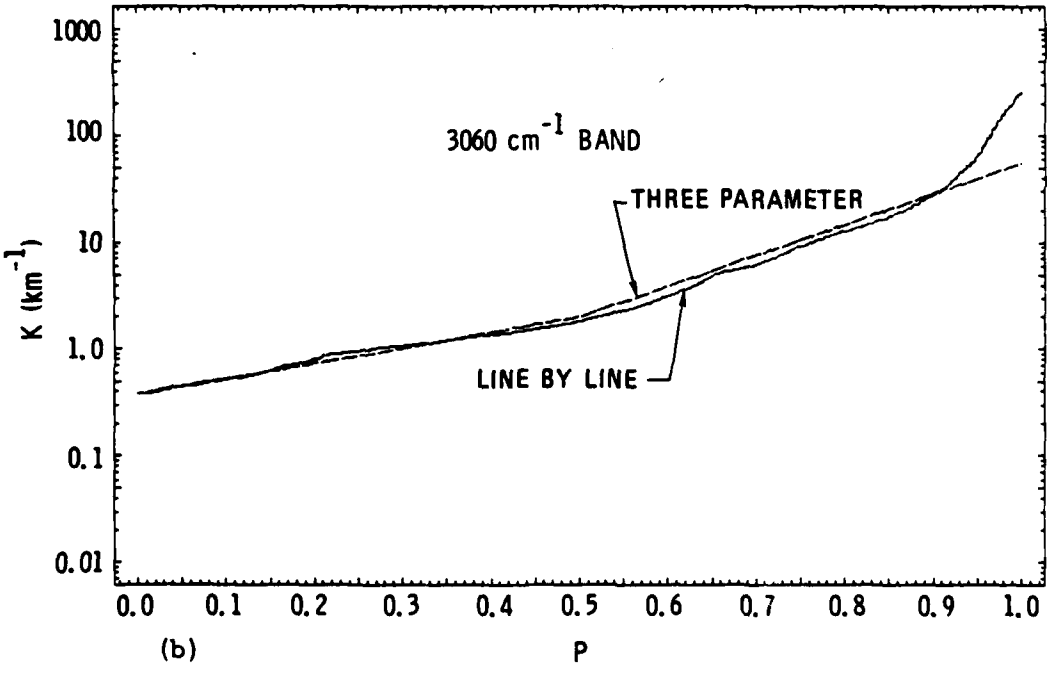

Fig. 21. Monotonic Absorption Function k(p). Comparison of line by line and three-parameter model.

The transmittance is obtained by substituting the expression for f(k) given by Eq. (48) into Eq. (33) and evaluating the integrals. The result is

$$\overline{T}(x) = \frac{1}{b_1}\left[E_1(k_0\, x) - E_1(k_{1/2}\, x)\right] + \frac{1}{b_2}\left[E_1(k_{1/2}\, x) - E_1(k_1\, x)\right] \qquad (54)$$

Using Eqs. (45) and (46) we can express b_1 and b_2 in terms of k_0, $k_{1/2}$, and k_1. The final form for our three-parameter formula is

$$\overline{T}(x) = \frac{1}{2\ \ell n(k_{1/2}/k_0)}\left[E_1(k_0\, x) - E_1(k_{1/2}\, x)\right]$$

$$+ \frac{1}{2\ \ell n(k_1/k_{1/2})}\left[E_1(k_{1/2}\, x) - E_1(k_1\, x)\right] \qquad (55)$$

Transmittances computed using this approximation are shown plotted in Figs. 22 and 23 along with the error curves. As can be seen, this three-parameter approximation is excellent over the entire range of distances.

In the discussion presented so far, the two-parameter and three-parameter approximations have been presented as approximations to line by line calculations. Obviously, they can also be used as a convenient fit to experimental transmittance data.

C. k-DISTRIBUTION FUNCTION

The function f(k) is defined by Eq. (34). In differential form it is

$$dp = f(k)\, dk \qquad (56)$$

Integrating this expression gives

$$\Delta p = p_2 - p_1 = \int_{k_1}^{k_2} f(k)\, dk \qquad (57)$$

The quantity Δp is the fraction of the spectral interval for which k is in the range $k_1 \leq k \leq k_2$. If k is considered to be a random variable, then f(k) is the probability density distribution of k and Δp is the probability that a

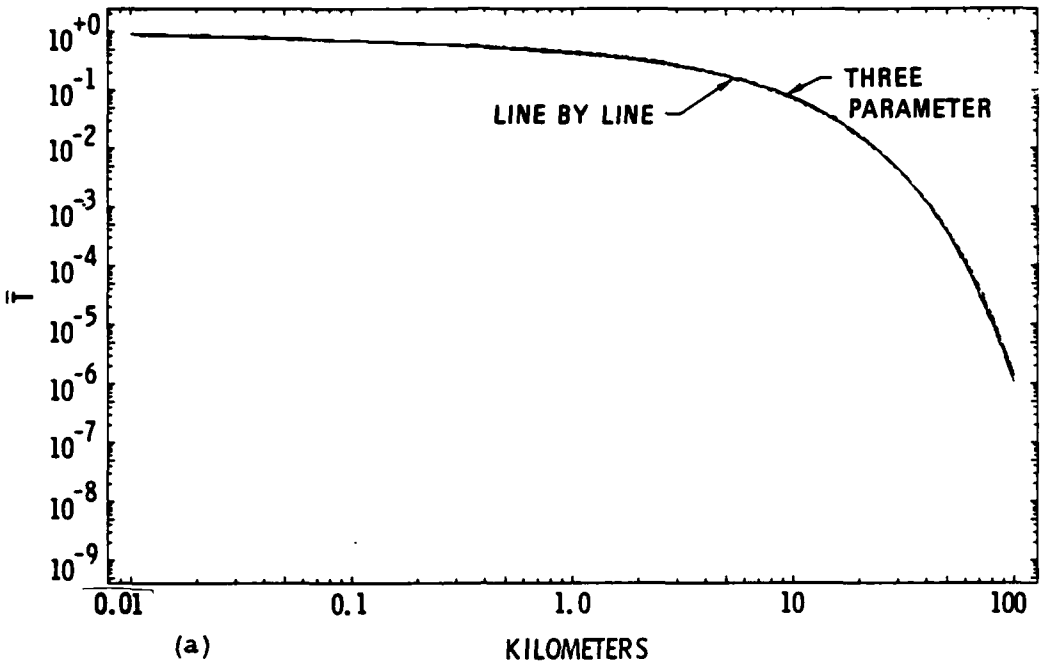

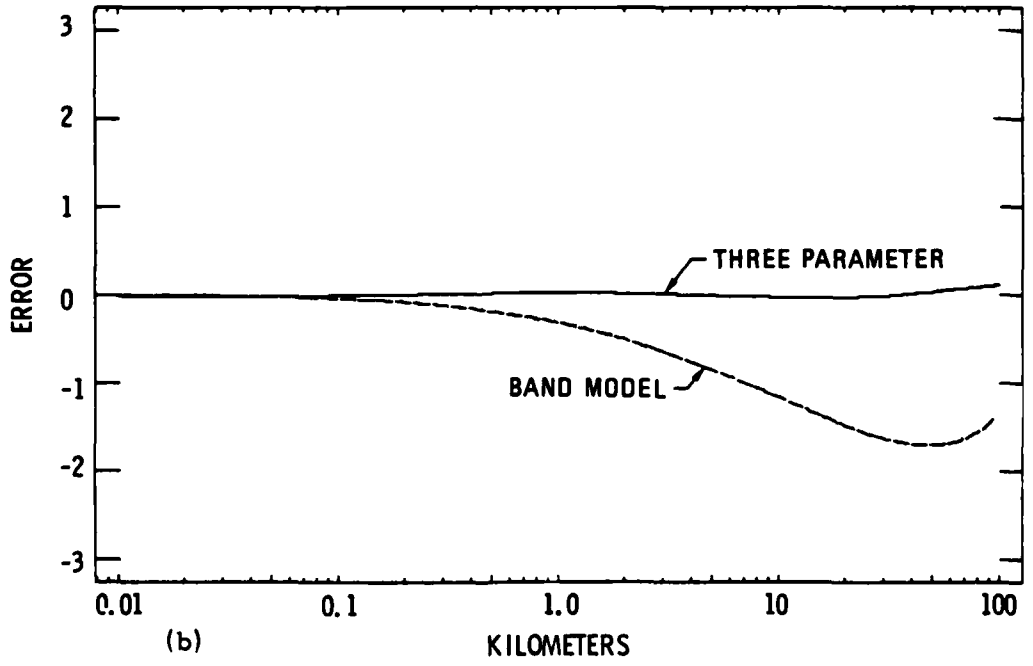

Fig. 22. Comparison of Line by Line ($\bar{T}_L$) and Three-Parameter Model ($\bar{T}_3$) Transmittances for 3040 cm^{-1} Band. Error = $Log_{10}(\bar{T}_3/\bar{T}_L)$. The band model error is also shown for comparison.

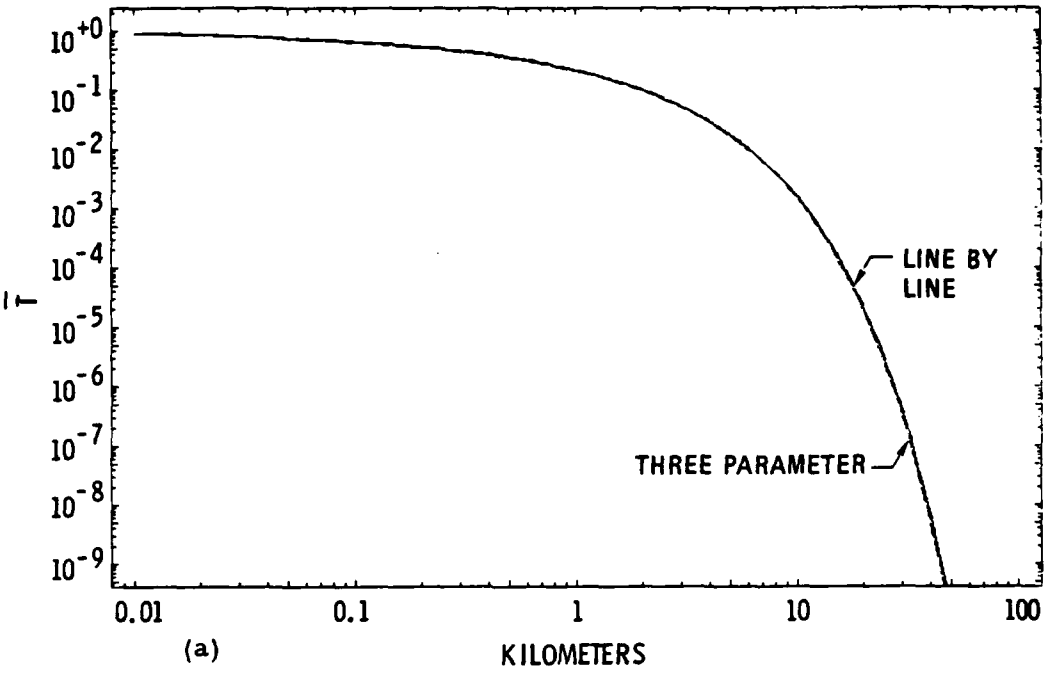

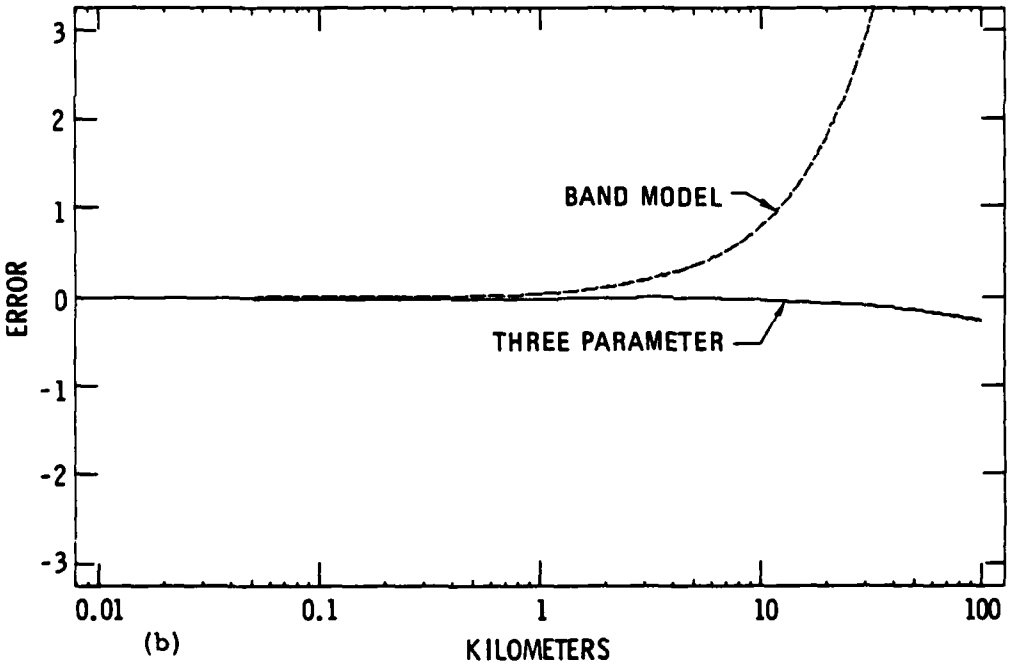

Fig. 23. Comparison of Line by Line ($\bar{T}_L$) and Three-Parameter Model ($\bar{T}_3$) Transmittances for 3060 cm^{-1} Band. Error = $Log_{10}(\bar{T}_3/\bar{T}_L)$. The band model error is also shown for comparison.

randomly chosen k will be in the interval $k_1 \leq k \leq k_2$. For this reason the function f(k) has been called by Arking and Grossman[5] the k-distribution function.

Given the k-distribution function f(k), the mean transmittance is given by Eq. (33). In this expression the lower and upper integration limits have been expressed as the finite values k_0 and k_1. This is in conformity with our expectations for real spectra where $k_0 > 0$ and $k_1 < \infty$. It will be useful now to extend these values to their ultimate limits and write

$$\overline{T}(x) = \int_0^\infty \exp[k\ x]\ f(k)\ dk \tag{58}$$

[This more general formula is true even for real spectra, since we only need to define f(k) = 0 outside the range $k_0 \leq k \leq k_1$.]

Domoto[7] recognized that this relation defines $\overline{T}(x)$ as the Laplace transform of f(k) and, conversely, f(k) is the inverse Laplace transform of $\overline{T}(x)$. He applied this procedure to the statistical band model where $\overline{T}(x)$ is given by Eq. (5). The inverse transform he obtained is

$$f(k) = \frac{1}{\bar{k}} \left[\frac{a}{\pi} \left(\frac{\bar{k}}{\bar{k}}\right)^3\right]^{1/2} \exp\left[a\left(2 - \frac{k}{\bar{k}} - \frac{\bar{k}}{k}\right)\right] \tag{59}$$

where $a = \bar{\gamma}/\delta_e$. This distribution is defined on the entire interval $0 \leq k < \infty$.

The k-distributions f(k) for the two and three parameter models are given by Eqs. (37) and (48), respectively. The exact k-distribution can be computed numerically from a line by line calculation. These functions are plotted in Figs. 24 and 25. Figure 24 compares a band model, line by line and the two-parameter model. Figure 25 is the same, but plots f(k) for the three-parameter model instead of the two-parameter model. Note that the three-parameter f(k) is discontinuous.

---

[7] G. Domoto, J. Quant. Spectrosc. Radiat. Transfer 14, 935 (1974).

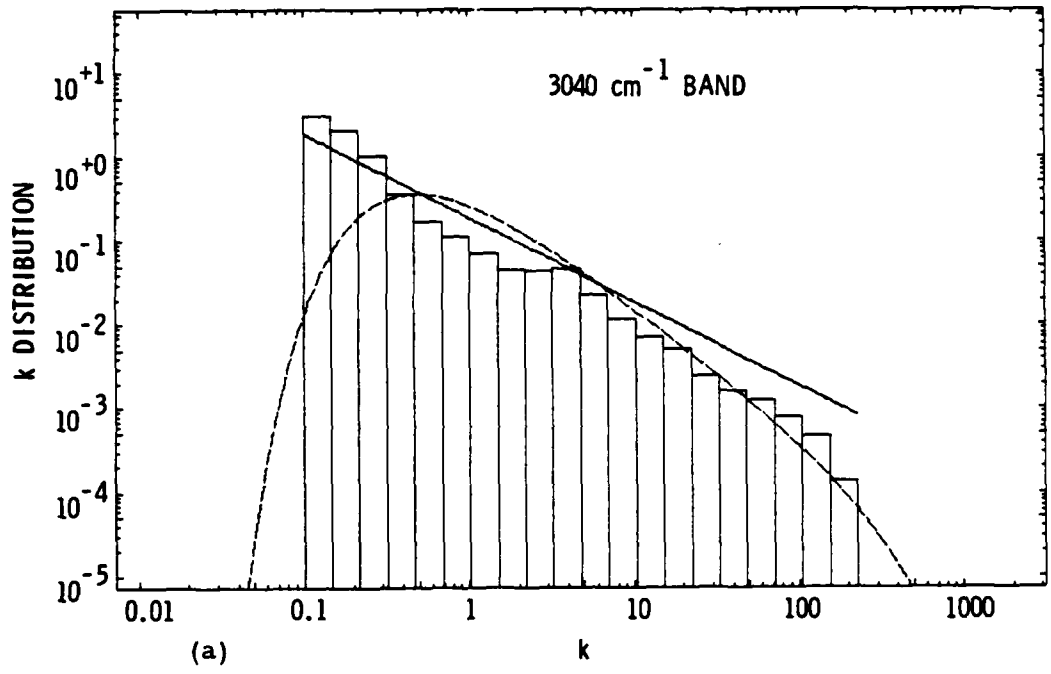

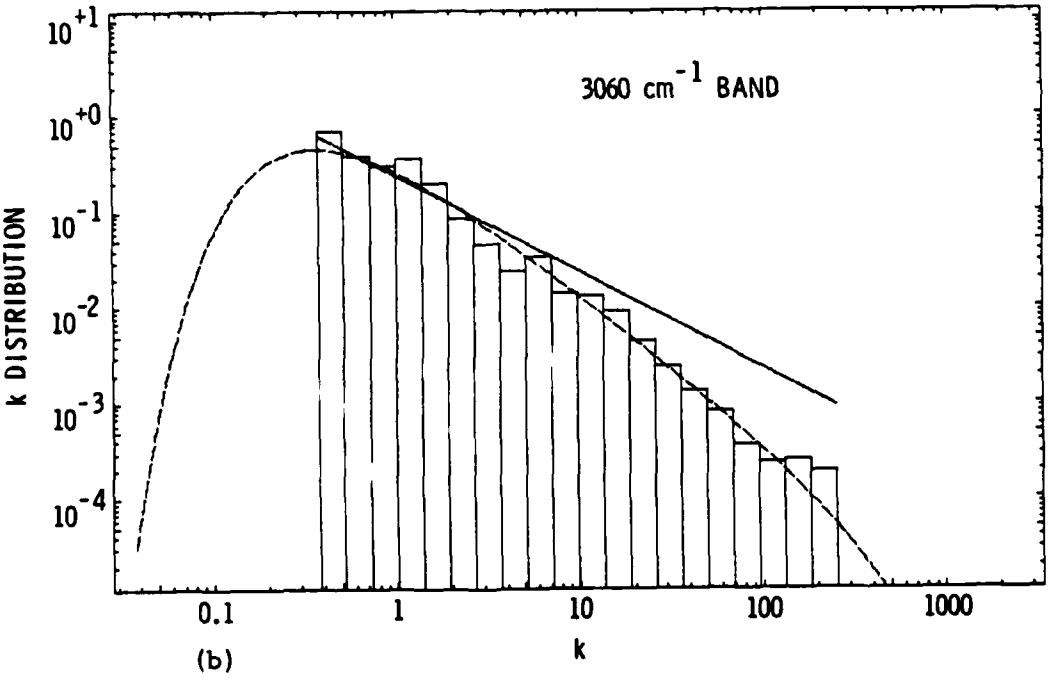

Fig. 24. k-Distribution Functions. Histogram is the line by line result, the dashed curve is the band model, and the solid line is the two-parameter model.

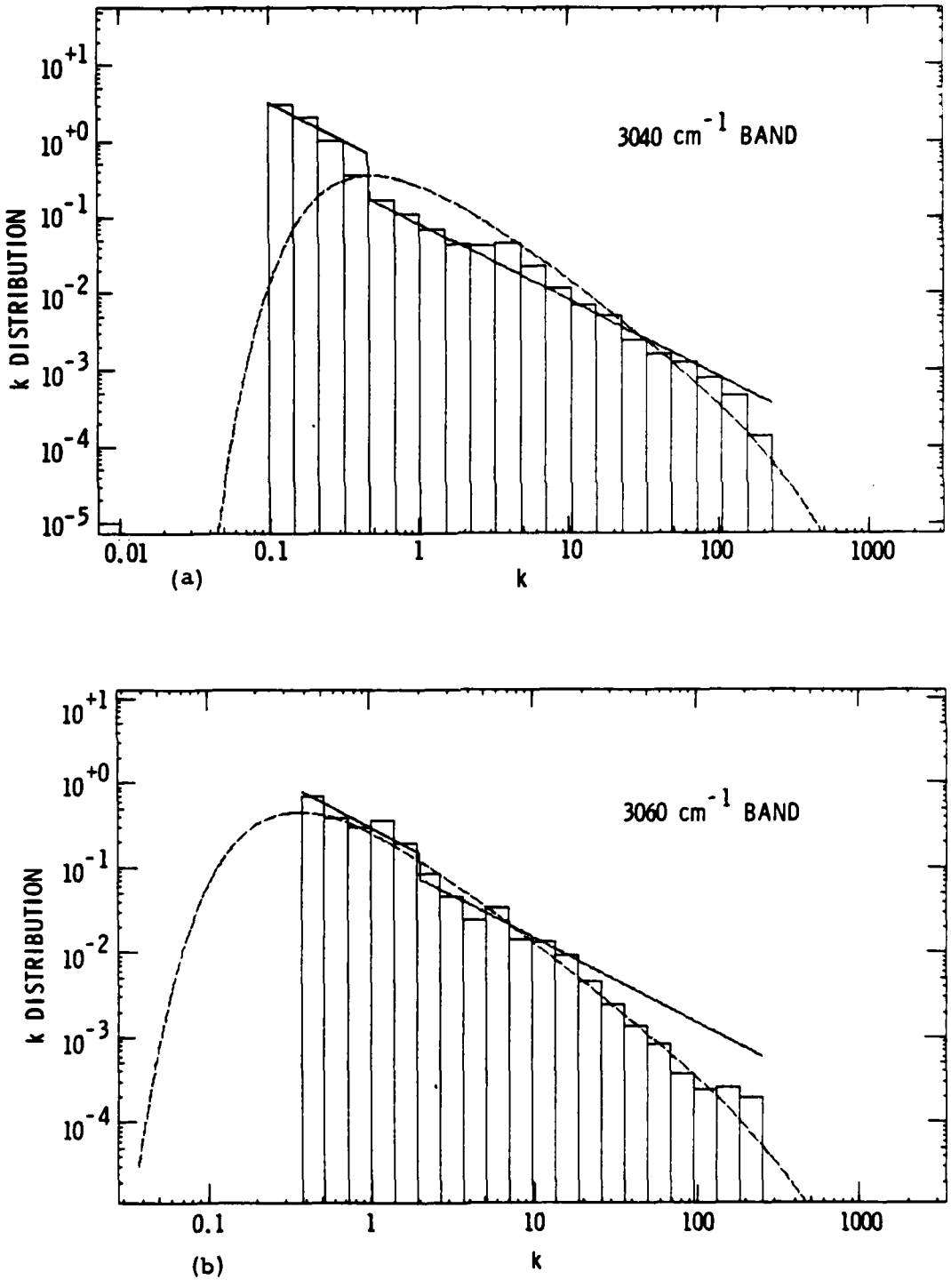

Fig. 25. k-Distribution Functions. Same as Fig. 24 except that the solid line is the three-parameter model.

The cumulative distribution function is obtained by integrating the probability density function[8]

$$p = \int_{k_{min}}^{k} f(k')\, dk' = F(k) \tag{60}$$

The inverse of this cumulative probability function is the function we have previously defined as the "monotonic absorption function" k(p). Thus

$$k(p) = F^{-1}(p) \tag{61}$$

This procedure provides a means of computing the monotonic absorption function k(p) for the statistical band model. Both steps of the procedure must be done numerically: first a numerical integration of f(k) to obtain F(k) and then a numerical interpolation to obtain $F^{-1}(p)$. The results are plotted in Fig. 26. The exact results are also plotted for comparison. This graph should be compared with Figs. 15, 18, and 21, where k(p) for the two- and three-parameter models are plotted.

The functions $\overline{T}(x)$ and k(p) are transforms of each other. One can be computed from the other. The function k(p) is calculated from $\overline{T}(x)$ by the procedure just outlined and $\overline{T}(x)$ is calculated from k(p) by Eq. (26). The behavior of $\overline{T}(x)$ for large values of x is determined, for the most part, by the values of k(p) in the interval near p = 0. This is illustrated in Fig. 15 where the upper limit of integration used in Eq. (26) to calculate 90% of the final value of $\overline{T}(x)$ is plotted for various values of x. In the limit as $x \to \infty$, $\overline{T}(x)$ is determined by the single point at p = 0, $k(0) = k_{min}$ [see Eq. (22)]. Thus, in order to compute $\overline{T}(x)$ accurately for large optical path lengths, it is necessary to have an accurate approximation of the function k(p) at and near p = 0.

[8] S. L. Meyer, Data Analysis for Scientists and Engineers, Wiley, New York (1975) p. 20, 103.

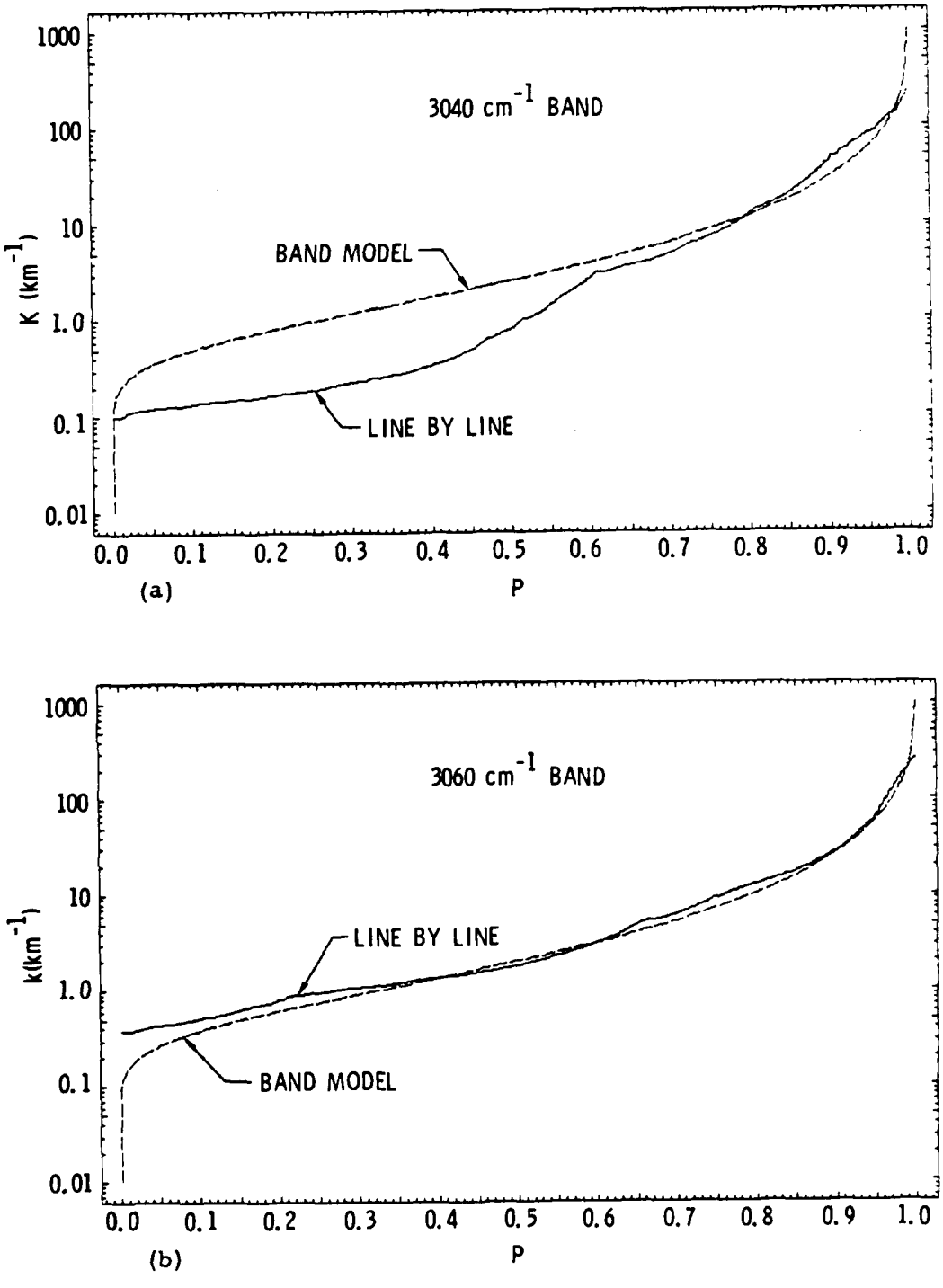

Fig. 26. Monotonic Absorption Function k(p). Comparison of line by line and band model. Compare this also with Figs. 15, 18, and 21.

The two- and three-parameter approximations we have proposed take advantage of the relatively simple form of the function k(p) by approximating ln[k(p)] by one or two straight line segments. These approximations are constrained to be equal to k_{min} at p = 0. This ensures that our approximation will have the correct long range behavior.

The statistical band model, on the other hand, is basically limited in accuracy for large values of x because the information contained in the band model parameters $\bar{k}$, $\bar{\gamma}$, and δ_e is not sufficient to determine k_{min}. More generally it is not sufficient to determine k(p) in the interval near p = 0. The best that can be done with this information is to determine a distribution of $k_\alpha(p)$ functions which are compatible with the parameters. (The subscript α labels the functions in this distribution.) The functions $k_\alpha(p)$ determine a family of mean transmittance functions $\bar{T}_\alpha(x)$. These in turn determine a family of error curves $E_\alpha(x)$, which will look very much like the family of error curves shown in Fig. 14.*

If the only information we are given about a band is the statistical band model parameters, then each of the error curves $E_\alpha(x)$ is equally probable. The error curve that applies in any particular case can be thought of as just a random selection from this family of curves.

Before leaving this section, it is interesting to examine the functions k(p) plotted in Fig. 26 in more detail. For convenience, the band model function will be written $k_B(p)$ and the line by line function will be written as $k_L(p)$. The general behavior of $k_B(p)$ is that it turns sharply downward near p = 0 and approaches the value $k_B(0) = 0$, which is always less than $k_{min} = k_L(0)$. This is a manifestation of the incorrect asymptotic form of the band model transmittance function given by Eq. (21).

*The family of error curves shown in Fig. 15 is not exactly the same as those described here. In Fig. 15 the parent populations were fixed, whereas in the case decribed here the band model parameters k, $\bar{\gamma}$, and δ_e are held constant. After the calculations for this report were complete, we discovered a simple method to generate line parameters that have fixed band model parameters. However, we believe that the family of error curves shown in Fig. 15 is at least a good qualitative and also a semiquantitative picture of the behavior that would result when the band model parameters are held fixed.

In the region $0 \leq p \leq p_2$ where $p_2 \sim 0.5$, the relationship between $k_B(p)$ and $k_L(p)$ will generally be one of two types. Either $k_B(p) < k_L(p)$ as in the lower graph of Fig. 26 or $k_B(p)$ and $k_L(p)$ will intersect at some small value p_1 with $k_B(p) > k_L(p)$ in the region $p_1 \leq p \leq p_2$ as in the upper graph of Fig. 26. For the first case, we can predict from Eq. (26) that $\overline{T}_B(x) > \overline{T}_L(x)$ and thus the error ratio will be greater than 1. This behavior is illustrated in Fig. 3b.

In the second case, the behavior is more complicated. For moderate values of x the result will be $\overline{T}_B(x) < \overline{T}_L(x)$. However, as x increases, the effective range of integration in Eq. (26) decreases. At some point it will fall entirely within the interval $0 \leq p \leq p_1$ where $k_B(p) < k_L(p)$. When this occurs we obtain $\overline{T}_B(x) > \overline{T}_L(x)$. Thus the functions $\overline{T}_L(x)$ and $\overline{T}_B(x)$ eventually cross and the error ratio varies from less than 1 to greater than 1. The beginning of this behavior is illustrated in Fig. 2b which presumably would follow the scenario just outlined if x were extended beyond 100 km. The error curves shown in Fig. 14 illustrate both types of behavior.

D. *MONTE CARLO METHOD*

The term "Monte Carlo" usually refers to a computational procedure in which a large (or infinite) distribution of values of some quantity or parameter is replaced by a manageably small, unbiased random sample of the distribution. For example, a physical quantity may be the average value of some distribution. The Monte Carlo approximation is computed by generating a random sample of the distribution and then averaging the random sample. In the present case, the Monte Carlo method is a practical procedure for calculating the parameters for the two- and three-parameter approximations from an unbiased random sample of the k-distribution.

The k-distribution is the continuously infinite collection (or population) of k values that are defined by the function $k(\nu)$ in the band interval $\Delta\nu$ without regard to their order. An unbiased random sample of this infinite population of k values can be generated by randomly selecting M wave

numbers ν_i (i = 1, M) from the band interval and then calculating $k(\nu_i)$ using Eq. (2). The random wave numbers are computed from random numbers X_i in the interval 0 to 1 by the formula

$$\nu_i = (\nu_U - \nu_L)\, X_i, \quad i = 1, M \tag{62}$$

where ν_U and ν_L are the upper and lower boundaries of the band.

The least value of k in this random sample is a good approximation to k_{min} and is set equal to the parameter k_0 for both the two- and three-parameter approximations.

The average value of $\ell n(k)$ for the M values of k in the random sample is the Monte Carlo approximation to the quantity $\langle \ell n(k) \rangle$ defined by Eq. (41). The parameter k_1 for the two-parameter approximation is then calculated by combining Eqs. (35) and (43) to obtain

$$k_1 = \frac{1}{k_0} \exp[2\, \langle \ell n(k) \rangle] \tag{63}$$

For the three-parameter model *we must compute* Monte Carlo approximations for the quantities $\langle \ell n(k) \rangle_1$ and $\langle \ell n(k) \rangle_2$ defined by Eqs. (50) and (51), respectively. The quantity k(p=1/2) is the median value of k which we designate k_{med}. This is the value of k such that half the elements of the distribution exceed it in value and half are less in value. The quantity $\langle \ell n(k) \rangle_1$ is the average value on $\ell n(k)$ for $k < k_{med}$ and $\langle \ell n(k) \rangle_2$ is the average value of $\ell n(k)$ for $k > k_{med}$. Thus in the Monte Carlo approximation we divide the random sample of M elements into two groups, each with M/2 elements such that any k value in the first group is less than any k value in the second group. (In order to avoid any ambiguities in this procedure, we always choose M to be an even integer.) The average value of $\ell n(k)$ in the first group is an approximation to $\langle \ell n(k) \rangle_1$ and the average value of $\ell n(k)$ in the second group approximates $\langle \ell n(k) \rangle_2$. The parameters $k_{1/2}$ and k_1 for the three-parameter model are then computed by combining Eqs. (45), (46), (52), and (53) to obtain

$$k_{1/2} = \frac{1}{k_0} \exp[4 \langle \ell n(k) \rangle_1] \tag{64}$$

and

$$k_1 = \frac{1}{k_{1/2}} \exp[4\langle \ell n(k) \rangle_2] \tag{65}$$

In Figs. 27 and 28 we show the results obtained by this method using the three-parameter approximation and a random sample of M = 50 values of k. These results are almost as good as the results obtained previously using 1000 points but required about 1/20 the computational effort. The Monte Carlo procedure is thus an efficient method for carrying out (approximate) line by line calculations.

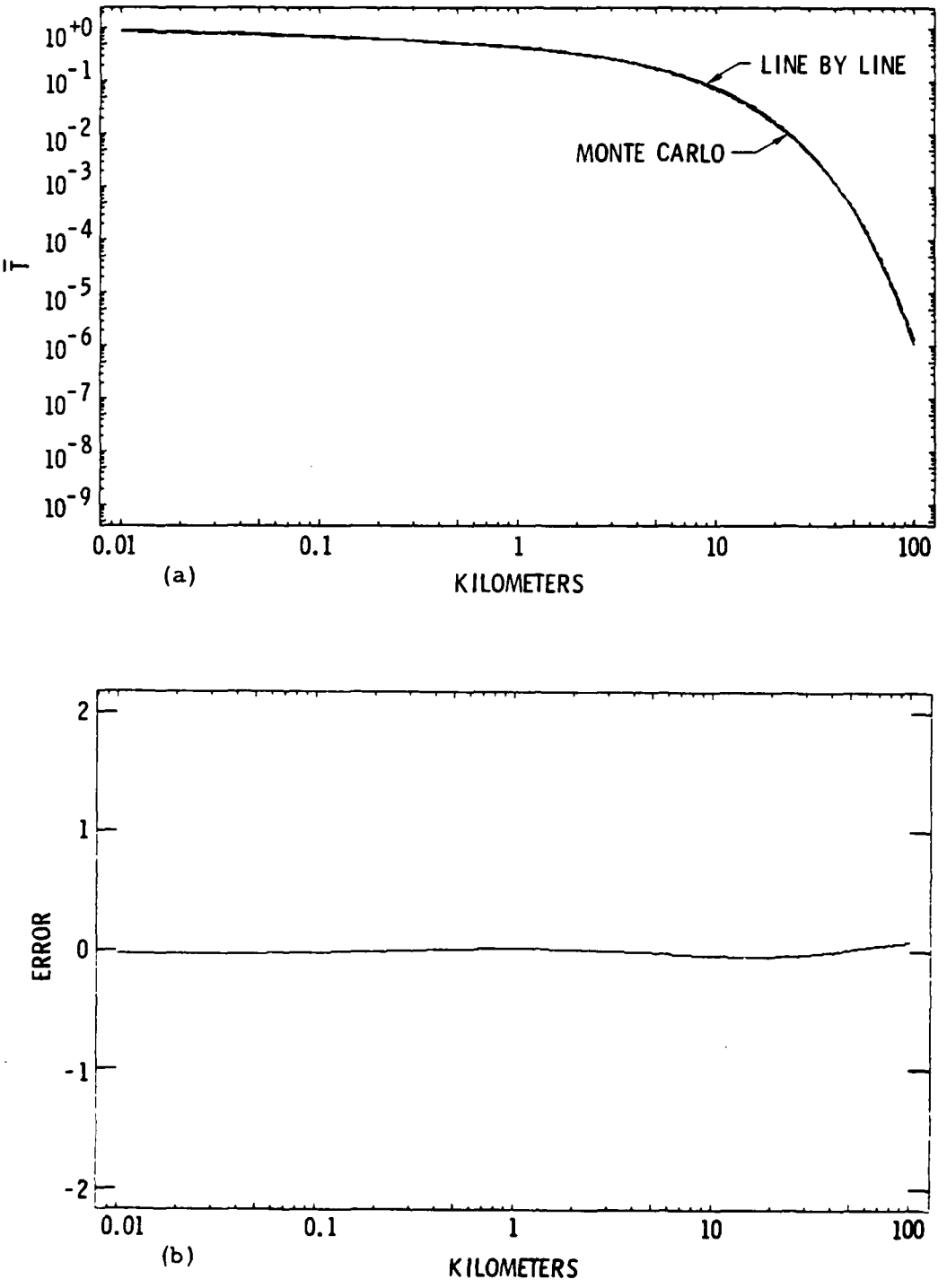

Fig. 27. Comparison of Line by Line ($\bar{T}_L$) and 50 Point Monte Carlo ($\bar{T}_{50}$) Transmittances for 3040 cm^{-1} Band. Error = $Log_{10}(\bar{T}_{50}/\bar{T}_L)$.

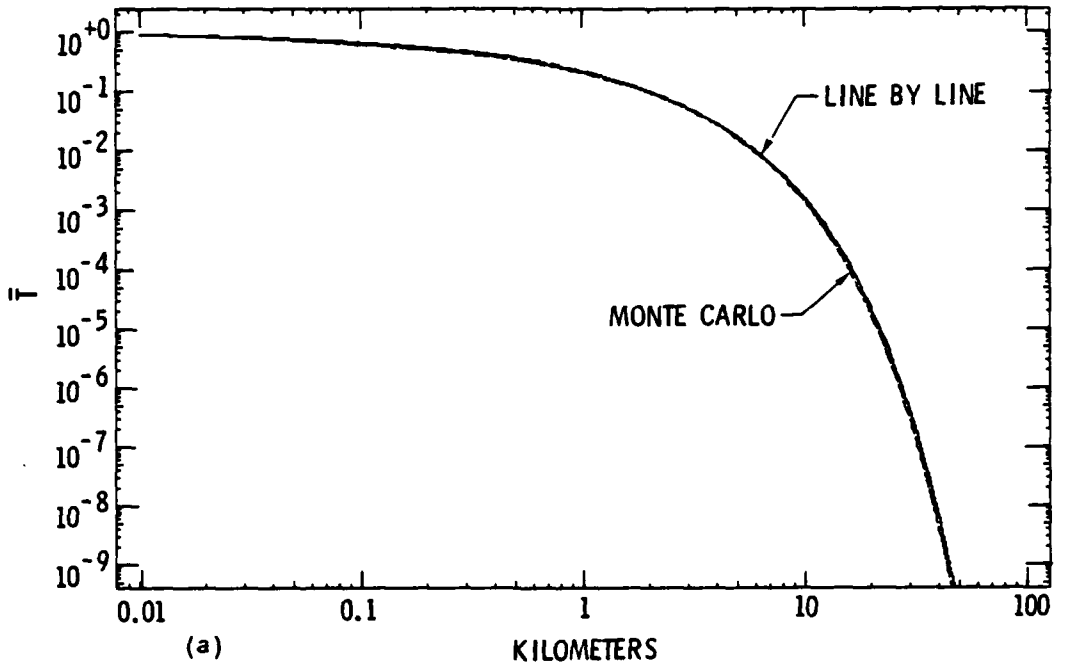

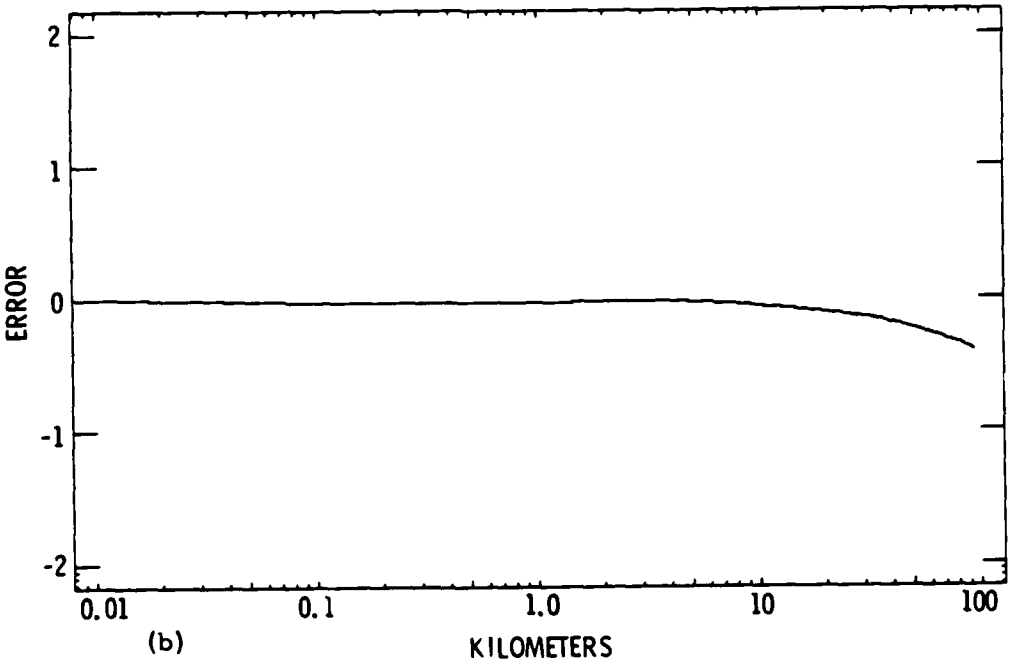

Fig. 28. Comparison of Line by Line ($\bar{T}_L$) and 50 Point Monte Carlo ($\bar{T}_{50}$) Transmittances for 3060 cm^{-1} Band. Error = $Log_{10}(\bar{T}_{50}/\bar{T}_L)$.

IV. SUMMARY AND DISCUSSION

In this report, we have investigated the reliability of the statistical band model by comparing the model with precise line by line calculations, and we have also derived two new nonstatistical band model approximations.

The first part of the study, which is an evaluation of the statistical band model, is contained mainly in Section II with some additional discussion in III-C. The study was carried out on a system of H_2O absorbers in the wave number range 2800 to 3400 cm^{-1}. Tests were also made using sets of computer generated line parameters. The results of these calculations were presented graphically.

Figures 5 and 6 show that the distribution of H_2O line strengths and line spacings are in reasonable agreement with the theoretical assumptions made in the statistical band model. The line by line and band model transmittances are compared in Figs. 1, 2, 3, 13, and 14. It is concluded from these (and others not presented here) that the statistical band model is fairly reliable in the short optical path length regime in which $\overline{T}(x) > 0.1$, but for long paths where $\overline{T}(x) < 0.1$, the transmittances can be in serious error by orders of magnitude. This error has a random component that dominates at intermediate distances and a systematic component that dominates at very long distances.

The random error arises because the information contained in the band model parameters is not sufficient to define a unique k-distribution, but rather is compatible with an entire ensemble of k-distributions from which one has been randomly selected.

The systematic error arises because of certain simplifying assumptions made in the derivation of the band model transmittance. All values of the strength parameter and all values of line spacing from 0 to ∞ were allowed. As a result, the k-distribution extends from 0 to ∞ whereas any real distribution has finite limits, $k_{min} > 0$ and $k_{max} < \infty$. The unphysical k values in the range 0 to k_{min} result in an erroneous asymptotic behavior for the band model

transmittance that is consistently too large. This systematic component of the error is easily computed from the asymptotic formulas and is given in Eq. (23).

The second part of this report is concerned with the derivation and testing of two new nonstatistical band model approximations. They are referred to simply as the two-parameter and three-parameter approximations. The formulas for these two approximations are given by Eqs. (40) and (55). They are compared with the exact results and with the statistical band model in Figs. 19, 20, 22, and 23. We conclude that the two-parameter model is sometimes slightly inferior to the statistical band model for short optical paths but is always much superior for long paths. The three-parameter model is uniformly excellent for all path lengths.

The present study was a preliminary investigation and was limited in its scope. A more complete study should repeat most of the calculations in this report over a broader range of conditions including much higher and lower temperatures and pressures, for other portions of the H_2O line system, and for several other molecules, especially CO_2. Also other line profiles should be studied.

Several other topics that could be included in a new study would be a study of the temperature and pressure dependence of the model parameters k_0, $k_{1/2}$, and k_1; a generalization of our new approximations to systems with nonuniform temperatures and pressures; and the development of practical numerical techniques for fitting both the two- and three-parameter formulas to experimental transmittance data.

REFERENCES

1. L. S. Rothmon, Appl. Opt. 20, 791 (1981).

2. A. Goldman and T. Kyle, Appl. Opt. 7, 1167 (1968).

3. S. J. Young, Band Model Parameters for the 2.7- μm Bands of H_2O and CO_2 in the 100 to 3000° K Temperature Range, TR-0076(6970)-4, The Aerospace Corp. (31 July 1975).

4. W. Malkmus, J. Opt. Soc. Am. 57, 323 (1967).

5. A. Arking and K. Grossman, J. Atmos. Sci. 29, 937 (1972).

6. M. Abramowitz and I. Stegun, Handbook of Mathematical Functions, Dover, New York (1965).

7. G. Domoto, J. Quant. Spectrosc. Radiat. Transfer 14, 935 (1974).

8. S. L. Meyer, Data Analysis for Scientists and Engineers, Wiley, New York (1975) p. 20, 103.

LABORATORY OPERATIONS

The Laboratory Operations of The Aerospace Corporation is conducting experimental and theoretical investigations necessary for the evaluation and application of scientific advances to new military space systems. Versatility and flexibility have been developed to a high degree by the laboratory personnel in dealing with the many problems encountered in the nation's rapidly developing space systems. Expertise in the latest scientific developments is vital to the accomplishment of tasks related to these problems. The laboratories that contribute to this research are:

Aerophysics Laboratory: Launch vehicle and reentry aerodynamics and heat transfer, propulsion chemistry and fluid mechanics, structural mechanics, flight dynamics; high-temperature thermomechanics, gas kinetics and radiation; research in environmental chemistry and contamination; cw and pulsed chemical laser development including chemical kinetics, spectroscopy, optical resonators and beam pointing, atmospheric propagation, laser effects and countermeasures.

Chemistry and Physics Laboratory: Atmospheric chemical reactions, atmospheric optics, light scattering, state-specific chemical reactions and radiation transport in rocket plumes, applied laser spectroscopy, laser chemistry, battery electrochemistry, space vacuum and radiation effects on materials, lubrication and surface phenomena, thermionic emission, photosensitive materials and detectors, atomic frequency standards, and bioenvironmental research and monitoring.

Electronics Research Laboratory: Microelectronics, GaAs low-noise and power devices, semiconductor lasers, electromagnetic and optical propagation phenomena, quantum electronics, laser communications, lidar, and electro-optics; communication sciences, applied electronics, semiconductor crystal and device physics, radiometric imaging; millimeter-wave and microwave technology.

Information Sciences Research Office: Program verification, program translation, performance-sensitive system design, distributed architectures for spaceborne computers, fault-tolerant computer systems, artificial intelligence, and microelectronics applications.

Materials Sciences Laboratory: Development of new materials: metal matrix composites, polymers, and new forms of carbon; component failure analysis and reliability; fracture mechanics and stress corrosion; evaluation of materials in space environment; materials performance in space transportation systems; analysis of systems vulnerability and survivability in enemy-induced environments.

Space Sciences Laboratory: Atmospheric and ionospheric physics, radiation from the atmosphere, density and composition of the upper atmosphere, aurorae and airglow; magnetospheric physics, cosmic rays, generation and propagation of plasma waves in the magnetosphere; solar physics, infrared astronomy; the effects of nuclear explosions, magnetic storms, and solar activity on the earth's atmosphere, ionosphere, and magnetosphere; the effects of optical, electromagnetic, and particulate radiations in space on space systems.